

# Syntheses and $^1\text{H}$ NMR Spectroscopy of Rigid, Cofacially Aligned, Porphyrin–Bridge–Quinone Systems in Which the Interplanar Separations between the Porphyrin, Aromatic Bridge, and Quinone Are Less than the Sum of Their Respective van der Waals Radii

Peter M. Iovine, Matthew A. Kellett, Naomi P. Redmore, and Michael J. Therien\*

Contribution from the Department of Chemistry, University of Pennsylvania, Philadelphia, Pennsylvania 19104-6323

Received March 1, 2000. Revised Manuscript Received July 7, 2000

**Abstract:** Unusually rigid  $\pi$ -stacked porphyrin–spacer–quinone systems have been synthesized using an approach that enables extensive control over the nature of electronic interactions between donor, aromatic spacer, and acceptor. This new class of porphyrin-based structures is distinct from related assemblies designed to probe electronic interactions between cofacial  $\pi$ -stacked aromatics: the donor (D), spacer (Sp), and acceptor (A) components of the assembly are held fixed at sub van der Waals contact distances, restricting severely the range of dynamical processes that modulate typically the magnitude of inter-ring separation and the extent of the lateral shift between juxtaposed aromatic units in the condensed phase. NMR spectroscopic studies demonstrate that these structures manifest disparate shielding environments which distribute uniformly the aromatic  $^1\text{H}$  resonances for these diamagnetic D–Sp–A compounds over spectral windows that exceed 9.0 ppm.

## Introduction

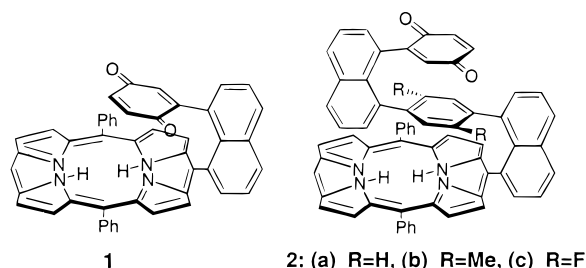
Fundamental issues regarding the role played by the medium (spacer) electronic structure in modulating donor–acceptor coupling in the charge tunneling regime, as well as the desire to control the magnitude of photoinduced charge separation and thermal charge recombination rate constants in synthetic donor–spacer–acceptor (D–Sp–A) systems, motivate the design of increasingly more complex electron transfer (ET) assemblies. Due to the long lifetimes and well characterized nature of both their electronically excited singlet and triplet states, porphyrinic components have figured prominently in such D–Sp–A assemblies; as a result, a plethora of synthetic approaches, including Diels–Alder cycloaddition,<sup>1–5</sup> condensation of appropriately substituted aldehydes and pyrroles,<sup>6–10</sup> self-assembly of complimentary H-bonding components,<sup>11–13</sup> and metal-catalyzed cross-coupling schemes,<sup>9,12,14</sup> have been applied to

the construction of elaborate porphyrin–spacer–quinone systems.<sup>15,16</sup> While there has been extensive interest in utilizing oligonucleotide-based scaffolds to build D–Sp–A complexes that feature stacked aromatic entities separating D from A,<sup>17–24</sup> constructs that manifest electronic interactions between cofacially aligned D, Sp, and A moieties that differ radically from deoxyribonucleic acid-based systems have yet to be developed. This is perhaps surprising, given the potential impact that both the magnitude of respective D, Sp, and A interplanar separations, and the nature of the quadrupolar interactions between these aromatics, may have on the regulation of the distance dependence of D–A electronic coupling in such cofacially organized  $\pi$  manifolds.<sup>25–27</sup>

- (1) Liddell, P. A.; Demanche, L. J.; Li, S. M.; Macpherson, A. N.; Nieman, R. A.; Moore, A. L.; Moore, T. A.; Gust, D. *Tetrahedron Lett.* **1994**, 35, 995–998.
- (2) Macpherson, A. N.; Liddell, P. A.; Lin, S.; Noss, L.; Seely, G. R.; DeGraziano, J. M.; Moore, A. L.; Moore, T. A.; Gust, D. *J. Am. Chem. Soc.* **1995**, 117, 7202–7212.
- (3) Lokan, N. R.; Craig, D. C.; Paddon-Row, M. N. *Synlett* **1999**, 4, 397–400.
- (4) Head, N. J.; Oliver, A. M.; Look, K.; Jones, G. A.; Paddon-Row, M. N. *Angew. Chem., Int. Ed.* **1999**, 38, 3219–3222.
- (5) Jolliffe, K. A.; Langford, S. J.; Oliver, A. M.; Shephard, M. J.; Paddon-Row, M. N. *Chem. Eur. J.* **1999**, 5, 2518–2530.
- (6) Lindsey, J. S.; Mauzerall, D. C. *J. Am. Chem. Soc.* **1982**, 104, 4498–4500.
- (7) Lindsey, J. S.; Delaney, J. K.; Mauzerall, D. C.; Linschitz, H. *J. Am. Chem. Soc.* **1988**, 110, 3610–3621.
- (8) Osuka, A.; Zhang, R. P.; Maruyama, K.; Yamazaki, I.; Nishimura, Y. *Bull. Chem. Soc., Jpn.* **1992**, 65, 2807–2813.
- (9) Wynne, K.; LeCours, S. M.; Galli, C.; Therien, M. J.; Hochstrasser, R. M. *J. Am. Chem. Soc.* **1995**, 117, 3749–3753.
- (10) Higashida, S.; Tsue, H.; Sugiura, K.; Kaneda, T.; Sakata, Y.; Tanaka, Y.; Taniguchi, S.; Okada, T. *Bull. Chem. Soc., Jpn.* **1996**, 69, 1329–1335.

- (11) Sessler, J. L.; Wang, B.; Harriman, A. *J. Am. Chem. Soc.* **1993**, 115, 10418–10419.
- (12) De Rege, P. J. F.; Williams, S. A.; Therien, M. J. *Science* **1995**, 269, 1409–1413.
- (13) Hayashi, T.; Miyahara, T.; Kumazaki, S.; Ogoshi, H.; Yoshihara, K. *Angew. Chem., Int. Ed. Engl.* **1996**, 35, 1964–1966.
- (14) Hyslop, A. G.; Kellett, M. A.; Iovine, P. M.; Therien, M. J. *J. Am. Chem. Soc.* **1998**, 120, 12676–12677.
- (15) Wasielewski, M. R. *Chem. Rev.* **1992**, 92, 435–461.
- (16) Piotrowiak, P. *Chem. Soc. Rev.* **1999**, 28, 143–150.
- (17) Purugganan, M. D.; Kumar, C. V.; Turro, N. J.; Barton, J. K. *Science* **1988**, 241, 1645–1649.
- (18) Murphy, C. J.; Arkin, M. R.; Jenkins, Y.; Ghatlia, N. D.; Bossmann, S. H.; Turro, N. J.; Barton, J. K. *Science* **1993**, 262, 1025–1029.
- (19) Meade, T. J.; Kayyem, J. F. *Angew. Chem., Int. Ed. Engl.* **1995**, 34, 352–354.
- (20) Arkin, M. R.; Stemp, E. D. A.; Holmlin, R. E.; Barton, J. K.; Hormann, A.; Olson, E. J. C.; Barbara, P. F. *Science* **1996**, 273, 475–480.
- (21) Lewis, F. D.; Wu, T.; Zhang, Y.; Letsinger, R. L.; Greenfield, S. R.; Wasielewski, M. R. *Science* **1997**, 277, 673–676.
- (22) Meggers, E.; Michel-Beyerle, M. E.; Giese, B. *J. Am. Chem. Soc.* **1998**, 120, 12950.
- (23) Meggers, E.; Kusch, D.; Spichty, M.; Wille, U.; Giese, B. *Angew. Chem., Int. Ed.* **1998**, 37, 460.
- (24) Fukui, K.; Tanaka, K. *Angew. Chem., Int. Ed.* **1998**, 37, 158–161.
- (25) Dougherty, D. A. *Science* **1996**, 271, 163–168.

We describe in this work the syntheses of *unusually* rigid  $\pi$ -stacked porphyrin–quinone (P–Q) systems via an approach that enables extensive control over the nature of electronic interactions between D, Sp, and A. This work exploits metal-mediated cross-coupling methodologies,<sup>28–35</sup> a valuable, new porphyrinic synthon,<sup>14</sup> and a 1,8-naphthyl pillaring motif, to provide entry into a new class of porphyrin-based supramolecular structures featuring cofacially aligned aromatic moieties fixed at sub van der Waals contact distances. The syntheses and spectacular 1-D <sup>1</sup>H NMR spectroscopic properties of four such species are reported, and include P–Q species, **1**, the prototype complex of this new family of D–Sp–A assemblies designed to probe the electronic coupling modulated through compressed, stacked  $\pi$  manifolds, along with tri-level systems **2a–c**, in which intervening phenyl, xylyl, and difluorophenyl units respectively separate the porphyrin and quinonyl moieties. These structures highlight the utility of this modular synthetic approach to generate supramolecular systems that manifest unusual electronic structures and demonstrate the ease at which bridge electronic structure can be modulated in this class of  $\pi$ -stacked D–Sp–A systems.



## Experimental Section

**Materials.** All manipulations were carried out under nitrogen previously passed through an O<sub>2</sub> scrubbing tower (Schweizerhall R3-11 catalyst) and a drying tower (Linde 3-Å molecular sieves) unless otherwise stated. Air-sensitive solids were handled in a Braun 150-M glovebox. Standard Schlenk techniques were employed to manipulate air-sensitive solutions. All solvents utilized in this work were obtained from Fisher Scientific (HPLC Grade). Tetrahydrofuran (THF), and 1,2-dimethoxyethane (DME) were predried over 4-Å molecular sieves and then distilled from Na/benzoylbiphenyl under N<sub>2</sub>, while CH<sub>2</sub>Cl<sub>2</sub> was distilled from CaH<sub>2</sub> under N<sub>2</sub>. Anhydrous dimethylformamide (DMF) (Aldrich Chemical Co.) was stirred over MgSO<sub>4</sub> prior to distillation under vacuum. Bis(pinacolato)diboron (Frontier Scientific) and halogenated reagents (Aldrich Chemical Co.) 1,4-dibromobenzene, 1,4-dibromo-2,5-dimethylbenzene, 1,4-dibromo-2,5-difluorobenzene were used as received. Ba(OH)<sub>2</sub>·8H<sub>2</sub>O (Aldrich Chemical Co.) was recrystallized from distilled H<sub>2</sub>O. The catalysts, Pd(PPh<sub>3</sub>)<sub>4</sub> and Pd(dppf)Cl<sub>2</sub>, were obtained from Strem. 1,8-Diiodonaphthalene was prepared using the procedure developed by House.<sup>36</sup> Chromatographic purification (Silica Gel 60, ICN 32–630) of all newly synthesized compounds was accomplished on the benchtop. Elemental analyses were performed

either at the Microanalytical Laboratory in the Department of Chemistry at the University of Pennsylvania or at Robertson Microtit Laboratories, Inc. (Madison, NJ).

**Instrumentation.** Electronic spectra were recorded on an OLIS UV/vis/NIR spectrophotometry system that is based on the optics of a Carey 14 spectrophotometer.

**NMR Data.** NMR Spectra were recorded on either a 500-MHz or AC 250-MHz Bruker spectrometer. Chemical shifts for <sup>1</sup>H NMR spectra are relative to TMS ( $\delta$  = 0.00 ppm); <sup>13</sup>C NMR spectra are referenced to deuteriochloroform solvent (CDCl<sub>3</sub>,  $\delta$  = 77.00 ppm), while those for <sup>19</sup>F NMR spectra are relative to fluorotrichloromethane (CCl<sub>3</sub>F,  $\delta$  = 0.00 ppm). The <sup>1</sup>H NMR spectra of compounds **8b**, **8c**, **9b**, **9c**, **10b**, **10c**, **2b**, and **2c** were recorded as diastereomeric mixtures; the *syn* and *anti* components of the mixture were not separable using the chromatographic media described above. <sup>1</sup>H NMR data for these compounds are therefore presented in the following manner: (i) resonances attributed to the *anti* isomer have their multiplicity labeled with a prime notation (') [e.g., (s', 3 H)], (ii) resonances attributed to the *syn* isomer have their multiplicity doubly primed (') [e.g., (s'', 3 H)], and (iii) resonances that correspond to overlapping signals of *syn* and *anti* isomers are denoted with unprimed notation [e.g., (s, 3 H)]. The diastereomeric ratio was determined by integration of well-resolved *anti* and *syn* resonances in the <sup>1</sup>H NMR spectrum. The specific *anti*/*syn* resonance pair utilized to determine a diastereomeric ratio varied from compound to compound.

**1,4-Di(4',4',5',5'-tetramethyl[1',3',2']dioxaborolan-2'-yl)benzene (7a).**<sup>37</sup> A 50 mL Schlenk reaction vessel was charged with pinacoldiboron ester (500 mg, 1.97 mmol), KOAc (263 mg, 2.68 mmol), and PdCl<sub>2</sub>(dppf) (20 mg, 0.027 mmol). A deoxygenated solution of 1,4-dibromobenzene (211 mg, 0.89 mmol) in DMF (10 mL) was cannula transferred into this flask; the mixture was heated at 80 °C for 2 h, and subsequently cooled, filtered, and partitioned with benzene and saturated aqueous NaCl. The organic layer was washed with saturated NaCl (3 × 75 mL) and H<sub>2</sub>O (1 × 50 mL), following which it was dried over CaCl<sub>2</sub>, and evaporated. The recovered dark solid was washed repetitively with 10 mL aliquots of cold *n*-pentane to remove unreacted pinacoldiboron. Sublimation of the crude solid in vacuo at 120 °C gives the product as a white crystalline material. Recrystallization of this material from hexanes affords pure white crystals; isolated yield = 93 mg (31% based on 211 mg 1,4-dibromobenzene); mp 235–236 °C. <sup>1</sup>H NMR (250 MHz, CDCl<sub>3</sub>):  $\delta$  7.80 (s, 4 H), 1.35 (s, 24 H). <sup>13</sup>C NMR (500 MHz, CDCl<sub>3</sub>):  $\delta$  24.84, 83.83, 133.88. HRMS (Cl<sup>+</sup>) *m/z*: 331.2252 (calcd for C<sub>18</sub>H<sub>29</sub>B<sub>2</sub>O<sub>4</sub> (MH<sup>+</sup>) 331.2252). Anal. Calcd for C<sub>18</sub>H<sub>28</sub>B<sub>2</sub>O<sub>4</sub>: C, 65.41; H, 8.55. Found: C, 65.31; H, 8.73.

**1,4-Dimethyl-2,5-di(4',4',5',5'-tetramethyl[1',3',2']dioxaborolan-2'-yl)benzene (7b).** A 50 mL Schlenk flask was charged with 1,4-dibromo-2,5-dimethylbenzene (2.0 g, 7.6 mmol), dioxaborolane (4.4 mL, 30 mmol), Et<sub>3</sub>N (6.3 mL, 45 mmol), and toluene (15 mL). This solution was degassed via three freeze–pump–thaw cycles, following which PdCl<sub>2</sub>(PPh<sub>3</sub>)<sub>2</sub> (319 mg, 0.45 mmol) was added. The reaction was heated at 80 °C for 12 h, cooled, and filtered. The solution was then diluted with additional benzene, washed with saturated NaCl (3 × 75 mL), H<sub>2</sub>O (1 × 50 mL), and subsequently dried over CaCl<sub>2</sub>, filtered, and evaporated, to give a tan solid. The crude material was refluxed in hexanes, filtered hot, and cooled to room temperature. The crystalline product was collected by vacuum filtration; isolated yield = 1.1 g (39% based on 2.0 g 1,4-dibromo-2,5-dimethylbenzene); mp > 250 °C. <sup>1</sup>H NMR (250 MHz, CDCl<sub>3</sub>):  $\delta$  7.52 (s, 2 H), 2.47 (s, 6 H), 1.32 (s, 24 H). <sup>13</sup>C NMR (500 MHz, CDCl<sub>3</sub>):  $\delta$  21.46, 24.87, 83.39, 136.90, 140.52. HRMS (Cl<sup>+</sup>) *m/z*: 359.2566 (calcd for C<sub>20</sub>H<sub>33</sub>B<sub>2</sub>O<sub>4</sub> (MH<sup>+</sup>) 359.2565). Anal. Calcd for C<sub>20</sub>H<sub>32</sub>B<sub>2</sub>O<sub>4</sub>: C, 66.99; H, 9.00. Found: C, 66.81; H, 9.09.

**1,4-Difluoro-2,5-di(4',4',5',5'-tetramethyl[1',3',2']dioxaborolan-2'-yl)benzene (7c).** A 50 mL Schlenk reaction vessel was charged with pinacoldiboron ester (616 mg, 2.4 mmol), KOAc (325 mg, 3.3 mmol), and PdCl<sub>2</sub>(dppf) (40 mg, 0.055 mmol). A deoxygenated solution of 1,4-dibromo-2,5-difluorobenzene (300 mg, 1.1 mmol) in DMF (10 mL) was cannula transferred into this flask; the mixture was heated at 80 °C for 15 h, and subsequently cooled, filtered, and partitioned with benzene and saturated aqueous NaCl. The organic layer was washed with saturated NaCl (3 × 75 mL) and H<sub>2</sub>O (1 × 50 mL) following

(26) Hunter, C. A.; Sanders, J. K. M. *J. Am. Chem. Soc.* **1990**, *112*, 5525–5534.

(27) Hunter, C. A. *Angew. Chem., Int. Ed. Engl.* **1993**, *32*, 1584–1586.

(28) Suzuki, A. *J. Organomet. Chem.* **1999**, *576*, 147–168.

(29) Miyaura, N.; Suzuki, A. *Chem. Rev.* **1995**, *95*, 2457–2483.

(30) Kumada, M. *Pure Appl. Chem.* **1980**, *52*, 669–679.

(31) Negishi, E.; Luo, F. T.; Frisbee, R.; Matsushita, H. *Heterocycles* **1982**, *18*, 117–122.

(32) Heck, R. F. *Acc. Chem. Res.* **1979**, *12*, 146–151.

(33) Stille, J. K. *Angew. Chem., Int. Ed. Engl.* **1986**, *25*, 508–524.

(34) DiMaggio, S. G.; Lin, V. S.-Y.; Therien, M. J. *J. Org. Chem.* **1993**, *58*, 5983–5993.

(35) DiMaggio, S. G.; Lin, V. S.-Y.; Therien, M. J. *J. Am. Chem. Soc.* **1993**, *115*, 2513–2515.

(36) House, H. O.; Koepsell, D. G.; Campbell, W. J. *J. Org. Chem.* **1972**, *37*, 1003–1011.

which it was dried over  $\text{CaCl}_2$ , and evaporated. The recovered dark solid was washed repetitively with 10 mL aliquots of cold *n*-pentane to remove unreacted pinacolboron. Sublimation of the crude solid in vacuo at 135 °C gives a white crystalline material. Recrystallization of this solid from hexanes affords pure white crystals of the product; isolated yield = 158 mg (39% based on 300 mg of 1,4-dibromo-2,5-difluorobenzene).  $^1\text{H}$  NMR (250 MHz,  $\text{CDCl}_3$ ):  $\delta$  7.33 (t, 2 H,  $J = 6.6$  Hz), 1.35 (s, 24 H).  $^{13}\text{C}$  NMR (500 MHz,  $\text{CDCl}_3$ ):  $\delta$  24.79, 84.27, 122.23, 122.34, 122.40, 122.50, 161.46, 161.49, 163.44, 163.48.  $^{19}\text{F}$  NMR (200 MHz,  $\text{CDCl}_3$ ):  $\delta$  -111.52 (s, 2 F). HRMS ( $\text{CI}^+$ )  $m/z$ : 367.2068 (calcd for  $\text{C}_{18}\text{H}_{27}\text{B}_2\text{F}_2\text{O}_4$  ( $\text{MH}^+$ ) 367.2064). Anal. Calcd for  $\text{C}_{18}\text{H}_{26}\text{B}_2\text{F}_2\text{O}_4$ : C, 58.98; H, 7.16. Found: C, 58.80; H, 7.03.

**1-Iodo-8-(2,5-dimethoxyphenyl)naphthalene (3).** A 1.0 M THF solution of (2,5-dimethoxyphenyl)magnesium bromide was prepared from 1-bromo-2,5-dimethoxybenzene and Mg turnings. The Grignard reagent (2.50 mL, 2.50 mmol) was diluted with THF (5 mL) in a 25 mL Schlenk flask and added dropwise to a solution of  $\text{ZnCl}_2$  (1.02 g, 7.5 mmol) in THF (15 mL). After the solution stirred for 15 min, a heavy white precipitate formed; the organozinc reagent was then transferred dropwise via cannula to a 100 mL Schlenk flask containing 1,8-diiodonaphthalene (1.00 g, 2.63 mmol) and  $\text{Pd}(\text{PPh}_3)_4$  (152 mg, 0.13 mmol) in THF (25 mL). The reaction was followed by TLC; after 12 h, no further changes were observed in the product distribution. Silica gel chromatography (19:1 hexanes:THF) yielded three fractions: residual 1,8-diiodonaphthalene, the desired mono-coupled product, and 1,8-bis(2,5-dimethoxyphenyl)naphthalene. The product was dissolved in ethanol (10 mL) and cooled to -38 °C, yielding a white precipitate, which was collected via filtration; isolated yield = 595 mg (61% based on 543 mg of 1-bromo-2,5-dimethoxybenzene): mp 97–99 °C.  $^1\text{H}$  NMR (250 MHz,  $\text{CDCl}_3$ ):  $\delta$  8.19 (dd, 1 H,  $J = 1.1$  Hz,  $J = 7.3$  Hz), 7.87 (m, 2 H), 7.47 (m, 2 H), 7.06 (t, 1 H,  $J = 7.7$  Hz), 6.96 (dd, 1 H,  $J = 3.0$  Hz,  $J = 8.8$  Hz), 6.85 (d, 1 H,  $J = 8.8$  Hz), 6.80 (d, 1 H,  $J = 3.0$  Hz), 3.79 (s, 3 H), 3.65 (s, 3 H).  $^{13}\text{C}$  NMR (500 MHz,  $\text{CDCl}_3$ ):  $\delta$  55.92, 56.02, 91.82, 111.64, 114.18, 118.47, 125.23, 126.28, 129.53, 129.96, 130.98, 131.09, 131.50, 135.07, 137.63, 142.03, 152.94, 153.39. HRMS ( $\text{ESI}^+$ )  $m/z$ : 390.011843 (calcd for  $\text{C}_{18}\text{H}_{15}\text{IO}_2$  ( $\text{M}^+$ ) 390.011682). Anal. Calcd for  $\text{C}_{18}\text{H}_{15}\text{IO}_2$ : C, 55.38; H, 3.88. Found: C, 55.53; H, 4.05.

**1-(2,5-Dimethoxyphenyl)-8-[4-(4',4',5',5'-tetramethyl[1',3',2']-dioxaborolan-2'-yl)-1-phenyl]naphthalene (8a).** A 25 mL Schlenk tube was charged with compound **3** (59 mg, 0.15 mmol),  $\text{K}_3\text{PO}_4$  (48 mg, 0.23 mmol), compound **7a** (100 mg, 0.30 mmol), and  $\text{Pd}(\text{PPh}_3)_4$  (9 mg,  $7.8 \times 10^{-3}$  mmol). DMF (5 mL), that had previously been deoxygenated via three freeze–pump–thaw cycles, was cannula transferred to the tube containing the solids. The reaction was heated at 100 °C for 2 h, cooled, filtered, and partitioned with benzene and saturated NaCl. The organic layer was washed with saturated NaCl (3  $\times$  75 mL) and  $\text{H}_2\text{O}$  (1  $\times$  50 mL), following which it was dried over  $\text{CaCl}_2$ , filtered, and evaporated, giving a light yellow solid. This material was chromatographed on silica gel ( $\text{CHCl}_3$ ). The product eluted after residual compound **3**; isolated yield = 40 mg (57% based on 59 mg of compound **3**).  $^1\text{H}$  NMR (250 MHz,  $\text{CDCl}_3$ ):  $\delta$  7.92 (d, 1 H,  $J = 8.1$  Hz), 7.91 (d, 1 H,  $J = 8.2$  Hz), 7.56–7.45 (m, 3 H), 7.36–7.33 (m, 2 H), 7.28 (d, 1 H,  $J = 7.1$  Hz), 7.16 (d, 1 H,  $J = 7.5$  Hz), 6.85 (d, 1 H,  $J = 7.7$  Hz), 6.55 (d, 1 H,  $J = 3.1$  Hz), 6.38 (dd, 1 H,  $J = 3.1$  Hz,  $J = 9.0$  Hz), 6.18 (d, 1 H,  $J = 9.0$  Hz), 3.68 (s, 3 H), 3.45 (s, 3 H), 1.35 (s, 6 H), 1.34 (s, 6 H).  $^{13}\text{C}$  NMR (500 MHz,  $\text{CDCl}_3$ ):  $\delta$  24.66, 24.96, 54.93, 55.86, 83.45, 110.32, 112.78, 117.96, 124.72, 125.07, 127.62, 128.66, 128.76, 129.87, 130.08, 130.12, 130.65, 132.69, 132.82, 132.95, 133.87, 134.82, 136.57, 140.82, 145.53, 150.00, 152.77. HRMS ( $\text{CI}^+$ )  $m/z$ : 467.2394 (calcd for  $\text{C}_{30}\text{H}_{32}\text{BO}_4$  ( $\text{MH}^+$ ) 467.2356).

**1-Iodo-8-[4-(8''-[2''', 5'''-dimethoxyphenyl]-1''-naphthyl)-1'-phenyl]naphthaene (9a).** A 25 mL Schlenk flask was charged with **8a** (38 mg, 0.082 mmol), 1,8-diiodonaphthalene (54 mg, 0.14 mmol),  $\text{Ba}(\text{OH})_2 \cdot 8\text{H}_2\text{O}$  (39 mg, 0.12 mmol), and  $\text{Pd}(\text{PPh}_3)_4$  (8 mg,  $6.9 \times 10^{-3}$  mmol). A degassed solution of dimethoxyethane (DME) (6 mL) and distilled water (1 mL) was cannula transferred to the reaction vessel. After heating at 80 °C for 1 h, the reaction mixture was partitioned with benzene and saturated NaCl. The organic layer was washed with saturated NaCl (3  $\times$  75 mL) and  $\text{H}_2\text{O}$  (1  $\times$  50 mL), following which it was dried over  $\text{CaCl}_2$ , filtered, and evaporated. The recovered oily

yellow residue was chromatographed on silica gel (9:1 hexanes:THF), giving a white solid; isolated yield = 17 mg (35% based on 38 mg of compound **8a**).  $^1\text{H}$  NMR (250 MHz,  $\text{CDCl}_3$ ):  $\delta$  8.18 (d, 1 H,  $J = 6.8$  Hz), 7.98–7.85 (m, 4 H), 7.60–7.51 (m, 3 H), 7.44 (dd, 1 H,  $J = 1.3$  Hz,  $J = 7.0$  Hz), 7.37 (dd, 2 H,  $J = 1.1$  Hz,  $J = 7.05$  Hz), 7.18 (d, 1 H,  $J = 7.6$  Hz), 7.08 (t, 1 H,  $J = 7.7$  Hz), 6.96–6.84 (m, 3 H), 6.62 (dd, 1 H,  $J = 3.0$  Hz,  $J = 8.7$  Hz), 6.58 (d, 1 H,  $J = 3.0$  Hz), 6.30 (d, 1 H,  $J = 8.7$  Hz), 3.67 (s, 3 H), 3.48 (s, 3 H).  $^{13}\text{C}$  NMR (500 MHz,  $\text{CDCl}_3$ ):  $\delta$  55.03, 55.78, 92.19, 110.34, 112.83, 117.59, 124.80, 125.03, 125.07, 126.45, 127.78, 128.60, 128.71, 128.79, 128.84, 129.67, 129.79, 130.03, 130.19, 130.40, 130.67, 130.75, 131.35, 133.25, 134.93, 135.43, 136.59, 138.01, 140.79, 141.99, 142.26, 142.34, 150.24, 152.65. HRMS ( $\text{CI}^+$ )  $m/z$ : 592.0898 (calcd for  $\text{C}_{34}\text{H}_{25}\text{IO}_2$  ( $\text{M}^+$ ) 592.0899).

**[5-(8'-(4''-(8'''-[2''', 5'''-Dimethoxyphenyl]-1''-naphthylaphthyl)-10,20-diphenylporphinato)zinc(II) (10a).** A 25 mL Schlenk tube was charged with **9a** (17 mg, 0.029 mmol), [5-(4',4',5',5'-tetramethyl[1',3',2']dioxaborolan-2'-yl)-10,20-diphenylporphinato]zinc(II) **4** (31 mg, 0.048 mmol),  $\text{Ba}(\text{OH})_2 \cdot 8\text{H}_2\text{O}$  (16 mg, 0.050 mmol), distilled  $\text{H}_2\text{O}$  (0.5 mL), and dimethoxyethane (DME) (5 mL). This solution was degassed via three freeze–pump–thaw cycles; following the addition of  $\text{Pd}(\text{PPh}_3)_4$  (3 mg, 0.0026 mmol), the mixture was heated at 80 °C for 1 h. After partitioning the reaction mixture with benzene and saturated NaCl, the organic layer was washed with saturated NaCl (3  $\times$  50 mL) and  $\text{H}_2\text{O}$  (1  $\times$  50 mL), dried over  $\text{CaCl}_2$ , filtered, and evaporated. The crude material was chromatographed on silica gel (17:3 hexanes:THF). A small fraction of (5,15-diphenylporphinato)zinc(II) eluted prior to the main product. The desired product eluted with a trace amount of an orange porphyrinic impurity; rechromatographing this material on silica gel gave pure compound **10a**; isolated yield = 23 mg (81% based on 17 mg of compound **9a**).  $^1\text{H}$  NMR (500 MHz,  $\text{CDCl}_3$ , see Figure 2 for proton labeling schematic):  $\delta$  10.15 (s, 1 H,  $\text{H}_{\text{meso}}$ ), 9.36 (d, 1 H,  $J = 4.5$  Hz,  $\text{H}_\beta$ ), 9.32 (d, 1 H,  $J = 4.4$  Hz,  $\text{H}_\beta$ ), 9.05 (d, 1 H,  $J = 4.4$  Hz,  $\text{H}_\beta$ ), 8.98 (d, 1 H,  $J = 4.4$  Hz,  $\text{H}_\beta$ ), 8.77 (d, 1 H,  $J = 4.6$  Hz,  $\text{H}_\beta$ ), 8.70 (d, 1 H,  $J = 4.6$  Hz,  $\text{H}_\beta$ ), 8.67 (d, 1 H,  $J = 4.6$  Hz,  $\text{H}_\beta$ ), 8.50 (d, 1 H,  $J = 4.6$  Hz,  $\text{H}_\beta$ ), 8.35 (d, 1 H,  $J = 7.1$  Hz,  $\text{H}_{11}$ ), 8.27 (d, 1 H,  $J = 6.8$  Hz,  $\text{H}_{14}$ ), 8.21–8.19 (m, 2 H,  $\text{H}_{13} + \text{H}_{\text{ortho}}$ , 10,20 phenyls), 8.17–8.14 (m, 2 H  $\text{H}_{\text{ortho}}$ , 10,20 phenyls  $\times$  2), 8.06 (d, 1 H,  $J = 7.3$  Hz,  $\text{H}_{\text{ortho}}$ , 10,20 phenyls), 7.82 (t, 1 H,  $J = 7.6$  Hz,  $\text{H}_{12}$ ), 7.74–7.67 (m, 6 H,  $\text{H}_{\text{meta/para}}$ , 10,20 phenyls), 7.60 (t, 1 H,  $J = 7.6$  Hz,  $\text{H}_{15}$ ), 7.25 (d, 1 H,  $J = 8.1$  Hz,  $\text{H}_8$ ), 6.98 (t, 1 H,  $J = 7.5$  Hz,  $\text{H}_9$ ), 6.88–6.87 (m, 2 H,  $\text{H}_{16} + \text{H}_7$ ), 6.64 (d, 1 H,  $J = 6.9$  Hz,  $\text{H}_{10}$ ), 6.20 (dd, 1 H,  $J = 3.1$  Hz,  $J = 8.8$  Hz,  $\text{H}_{17}$ ), 5.75 (d, 1 H,  $J = 8.8$  Hz,  $\text{H}_{18}$ ), 5.55 (d, 1 H,  $J = 3.0$  Hz,  $\text{H}_{19}$ ), 5.29 (dd, 1 H,  $J = 1.8$  Hz,  $J = 7.7$  Hz,  $\text{H}_2$ ), 5.18 (dd, 1 H,  $J = 1.8$  Hz,  $J = 7.7$  Hz,  $\text{H}_1$ ), 4.95 (t, 1 H,  $J = 7.6$  Hz,  $\text{H}_6$ ), 4.08 (dd, 1 H,  $J = 1.8$  Hz,  $J = 7.7$  Hz,  $\text{H}_4$ ), 3.86 (dd, 1 H,  $J = 1.8$  Hz,  $J = 7.7$  Hz,  $\text{H}_3$ ), 3.27 (s, 3 H,  $\text{OMe}$ ), 2.85 (s, 3 H,  $\text{OMe}$ ), 0.93 (d, 1 H,  $J = 7.0$  Hz,  $\text{H}_5$ ). Vis ( $\text{CH}_2\text{Cl}_2$ ): 423 (5.54), 467 (3.74), 547 (4.26), 584 (3.33). HRMS ( $\text{ESI}^+$ )  $m/z$ : 1011.2655 (calcd for  $\text{C}_{66}\text{H}_{44}\text{N}_4\text{O}_2\text{NaZn}$  ( $\text{M} + \text{Na}$ ) 1011.2653).

**[5-(8'-(2''-[2''', 5'''-Dimethoxyphenyl]-1'-naphthyl)-10,20-diphenylporphinato)zinc(II) (5).** A 50 mL Schlenk reaction vessel was charged with [5-(4',4',5',5'-tetramethyl[1',3',2']dioxaborolan-2'-yl)-10,20-diphenylporphinato]zinc(II) (250 mg, 0.26 mmol), **3** (100 mg, 0.26 mmol),  $\text{Ba}(\text{OH})_2 \cdot 8\text{H}_2\text{O}$  (122 mg, 0.38 mmol), distilled water (1.0 mL), and dimethoxyethane (DME) (10 mL). The solution was degassed via three freeze–pump–thaw cycles, following which  $\text{Pd}(\text{PPh}_3)_4$  (15 mg, 0.013 mmol) was added. The reaction mixture was heated at 80 °C for 6 h, quenched, and loaded onto a silica gel column (19:1 hexanes:THF). During the chromatographic separation, the eluent polarity was increased gradually to (9:1 hexanes:THF); a small fraction of (5,15-diphenylporphinato)zinc(II) eluted prior to the main product. After removal of the volatiles, the product was washed with hexanes and isolated via vacuum filtration on a fine glass frit; isolated yield = 185 mg (92% based on 100 mg of compound **3**).  $^1\text{H}$  NMR (250 MHz,  $\text{CDCl}_3$ , see Figure 3 for proton labeling schematic):  $\delta$  10.19 (s, 1 H,  $\text{H}_{\text{meso}}$ ), 9.39 (d, 1 H,  $J = 4.5$  Hz,  $\text{H}_\beta$ ), 9.36 (d, 1 H,  $J = 4.4$  Hz,  $\text{H}_\beta$ ), 9.07 (d, 1 H,  $J = 4.4$  Hz,  $\text{H}_\beta$ ), 9.05 (d, 1 H,  $J = 4.4$  Hz,  $\text{H}_\beta$ ), 8.92 (d, 1 H,  $J = 4.7$  Hz,  $\text{H}_\beta$ ), 8.80 (m, 2 H,  $\text{H}_\beta \times 2$ ), 8.56 (d, 1 H,  $J = 6.8$  Hz,  $\text{H}_1$ ), 8.47 (d, 1 H,  $J = 6.6$  Hz,  $\text{H}_{\text{ortho}}$ , 10,20 phenyls), 8.45 (d, 1 H,  $J = 4.5$  Hz,  $\text{H}_\beta$ ), 8.34 (m, 2 H,  $\text{H}_{\text{ortho}}$ , 10,20 phenyls +  $\text{H}_4$ ), 8.13 (d, 1 H,  $J = 8.2$  Hz,  $\text{H}_3$ ), 8.07 (d, 2 H,  $J = 6.9$  Hz,  $\text{H}_{\text{ortho}}$ , 10,20 phenyls  $\times$  2), 7.89 (t, 1 H,  $J =$



7.6 Hz, H<sub>2</sub>), 7.74 (m, 6 H, H<sub>meta/para</sub>, 10,20 phenyls), 7.45 (t, 1 H, *J* = 7.6 Hz, H<sub>5</sub>), 6.71 (d, 1 H, *J* = 7.0 Hz, H<sub>6</sub>), 4.88 (d, 1 H, *J* = 3.1 Hz, H<sub>C</sub>), 3.13 (d, 1 H, *J* = 9.0 Hz, H<sub>B</sub>), 2.43 (dd, 1 H, *J* = 3.1 Hz, *J* = 8.9 Hz, H<sub>A</sub>), 2.20 (s, 3 H, OMe), 1.26 (s, 3 H, OMe). <sup>13</sup>C NMR (500 MHz, CDCl<sub>3</sub>): δ 151.15, 150.09, 149.95, 149.70, 149.64, 149.55, 149.50, 149.26, 147.96, 142.97, 142.91, 139.34, 137.48, 135.59, 134.59, 134.51, 134.40, 133.97, 133.32, 133.25, 132.31, 132.07, 132.05, 131.77, 131.72, 131.43, 131.19, 130.86, 130.36, 130.28, 129.67, 128.79, 127.57, 127.40, 127.34, 126.72, 126.57, 126.48, 125.29, 123.26, 121.22, 120.82, 119.63, 114.90, 105.93, 105.53, 104.75, 53.59, 52.45. Vis (CH<sub>2</sub>Cl<sub>2</sub>): 423 (5.42), 549 (4.23). HRMS (FAB) *m/z*: 786.1973 (calcd for C<sub>50</sub>H<sub>34</sub>N<sub>4</sub>O<sub>2</sub>Zn (M<sup>+</sup>) 786.1996).

**5-[8'-(2'',5''-Benzoquinonyl)-1'-naphthyl]-10,20-diphenylporphyrin (1).** A 25 mL Schlenk reaction vessel was charged with **5** (31 mg, 0.039 mmol) and dry benzene (5 mL). Ten equivalents of BBr<sub>3</sub> (390 μL of a 1.0 M CH<sub>2</sub>Cl<sub>2</sub> solution, 0.39 mmol) were added dropwise to this solution. After stirring for 24 h at room temperature, the reaction mixture was diluted with additional benzene (5 mL), washed with saturated Na<sub>2</sub>CO<sub>3</sub> (3 × 50 mL) and H<sub>2</sub>O (1 × 50 mL), following which it was dried over CaCl<sub>2</sub>, filtered, and evaporated. The recovered red residue was chromatographed on silica gel (99:1 CH<sub>2</sub>Cl<sub>2</sub>:MeOH), affording a separation of two major bands. The first non-fluorescent band was the desired product **1**; the second band contained monodemethylated **6**. The combined fractions of **6** were concentrated to dryness and resubjected to the above reaction conditions; total isolated yield = 2 mg (7% based on 31 mg of compound **5**). <sup>1</sup>H NMR (500 MHz, CDCl<sub>3</sub>, see Figure 3 for proton labeling schematic): δ 10.19 (s, 1 H, H<sub>meso</sub>), 9.33 (d, 1 H, *J* = 4.9 Hz, H<sub>β</sub>), 9.30 (d, 1 H, *J* = 4.7 Hz, H<sub>β</sub>), 9.02 (d, 1 H, *J* = 4.9 Hz, H<sub>β</sub>), 8.97 (d, 1 H, *J* = 4.7 Hz, H<sub>β</sub>), 8.83 (d, 1 H, *J* = 5.1 Hz, H<sub>β</sub>), 8.61–8.60 (m, 3 H, H<sub>β</sub> + H<sub>ortho</sub>, 10,20 phenyls + H<sub>1</sub>), 8.58 (d, 1 H, *J* = 4.9 Hz, H<sub>β</sub>), 8.49 (d (br), 1 H, *J* = 8.1 Hz, H<sub>ortho</sub>, 10,20 phenyls), 8.36 (d, 1 H, *J* = 8.5 Hz, H<sub>4</sub>), 8.25 (d, 1 H, *J* = 4.9 Hz, H<sub>β</sub>), 8.20 (d, 1 H, *J* = 8.5 Hz, H<sub>3</sub>), 8.17 (d (br), 2 H, *J* = 7.7 Hz, H<sub>ortho</sub>, 10,20 phenyls), 7.96 (t, 1 H, *J* = 7.8 Hz, H<sub>2</sub>), 7.85–7.66 (m, 6 H, H<sub>meta/para</sub>, 10,20 phenyls), 7.48 (t, 1 H, *J* = 7.7 Hz, H<sub>5</sub>), 6.78 (d, 1 H, 7.0 Hz, H<sub>6</sub>), 4.97 (d, 1 H, *J* = 2.8 Hz, H<sub>C-Quinone</sub>), 2.02 (d, 1 H, *J* = 10.0 Hz, H<sub>B-Quinone</sub>), 1.65 (dd, 1 H, *J* = 2.8 Hz, *J* = 10.1 Hz, H<sub>A-Quinone</sub>), -3.35 (s (br), 2 H, N–H). UV–Vis (CH<sub>2</sub>Cl<sub>2</sub>): 414 (5.26), 500 (br) (3.92), 596 (3.66), 661 (3.39). HRMS (ESI<sup>+</sup>) *m/z*: 695.2454 (calcd for C<sub>48</sub>H<sub>31</sub>N<sub>4</sub>O<sub>2</sub> (M + H) 695.2454).

**5-[8'-(4''-[8'''-(2''',5'''-Benzoquinonyl)-1'''-naphthylthyl]-10,20-diphenylporphyrin (2a).** A dry CH<sub>2</sub>Cl<sub>2</sub> solution of **10a** (11 mg, 0.011 mmol) was cooled to -78 °C, following which 10 equivalents of BBr<sub>3</sub> (111 μL of a 1.0 M CH<sub>2</sub>Cl<sub>2</sub> solution, 0.11 mmol) were added dropwise. The reaction was stirred for 1 h at -78 °C and then slowly warmed to room temperature. After stirring for an additional h, a small quantity of methanol was added and the reaction stirred for 15 min. The reaction was then partitioned between CH<sub>2</sub>Cl<sub>2</sub> and saturated Na<sub>2</sub>CO<sub>3</sub>. The organic layer was washed with saturated Na<sub>2</sub>CO<sub>3</sub> (3 × 20 mL), dried, and filtered; PbO<sub>2</sub> (100 mg) was added, and the heterogeneous CH<sub>2</sub>Cl<sub>2</sub> solution was stirred for 1 h. After filtering and removal of the volatiles, the red material was chromatographed on silica gel (CH<sub>2</sub>Cl<sub>2</sub>). The quinonyl compound **2a** elutes first, followed by monodemethylated **10a**. After consolidation of the product fractions, **2a** was isolated as a glassy red solid; yield = 6.7 mg (67% based on 11 mg of compound **10a**). <sup>1</sup>H NMR (500 MHz, CDCl<sub>3</sub>, see Figure 2 for proton labeling schematic): δ 10.20 (s, 1 H, H<sub>meso</sub>), 9.36 (d, 1 H, *J* = 4.5 Hz, H<sub>β</sub>), 9.28 (d, 1 H, *J* = 4.5 Hz, H<sub>β</sub>), 8.99 (d, 1 H, *J* = 4.6 Hz, H<sub>β</sub>), 8.88 (d, 1 H, *J* = 4.3 Hz, H<sub>β</sub>), 8.71 (d, 1 H, *J* = 4.8 Hz, H<sub>β</sub>), 8.67 (d, 1 H, *J* = 4.7 Hz, H<sub>β</sub>), 8.58 (d, 1 H, *J* = 4.8 Hz, H<sub>β</sub>), 8.38 (d, 1 H, *J* = 7.7 Hz, H<sub>11</sub>), 8.35 (d, 1 H, *J* = 4.7 Hz, H<sub>β</sub>), 8.26–8.17 (m, 3 H, H<sub>14</sub> + H<sub>13</sub> + H<sub>ortho</sub>, 10,20 phenyls), 8.15 (d (br), 1 H, *J* = 6.8 Hz, H<sub>ortho</sub>, 10,20 phenyls), 8.09 (d (br), 1 H, *J* = 7.4 Hz, H<sub>ortho</sub>, 10,20 phenyls), 7.95 (d (br), 1 H, *J* = 7.4 Hz, H<sub>ortho</sub>, 10,20 phenyls), 7.83 (t, 1 H, *J* = 7.6 Hz, H<sub>12</sub>), 7.77–7.65 (m, 7 H, H<sub>15</sub> + H<sub>meta/para</sub>, 10,20 phenyls), 7.34 (d, 1 H, *J* = 8.2 Hz, H<sub>8</sub>), 6.99 (t, 1 H, *J* = 7.6 Hz, H<sub>9</sub>), 6.93 (d, 1 H, *J* = 6.8 Hz, H<sub>16</sub>), 6.85 (d, 1 H, *J* = 8.2 Hz, H<sub>7</sub>), 6.55 (d, 1 H, *J* = 6.6 Hz, H<sub>10</sub>), 6.11 (dd, 1 H, *J* = 2.6 Hz, *J* = 10.0 Hz, H<sub>17</sub>), 5.87 (d, 1 H, *J* = 7.5 Hz, H<sub>18</sub>), 5.76 (d, 1 H, *J* = 8.8 Hz, H<sub>1</sub>), 5.73 (d, 1 H, *J* = 7.6 Hz, H<sub>2</sub>), 5.49 (d, 1 H, *J* = 2.5 Hz, H<sub>19</sub>), 4.65 (t, 1 H, *J* = 7.7 Hz, H<sub>6</sub>), 4.23 (d, 1 H, *J* = 8.8 Hz, H<sub>4</sub>), 4.07 (d, 1 H, *J* = 7.2 Hz, H<sub>3</sub>), 0.62 (d, 1 H, *J* = 7.2 Hz, H<sub>5</sub>), -3.30 (s (br),

2 H, N–H). Vis (CH<sub>2</sub>Cl<sub>2</sub>): 422 (5.37), 516 (4.18), 550 (3.85), 590 (3.85), 648 (3.78). HRMS (ESI<sup>+</sup>) *m/z*: 919.3088 (calcd for C<sub>64</sub>H<sub>40</sub>N<sub>4</sub>O<sub>2</sub>-Na (M + Na) 919.3049).

**5-[8'-(2'',5''-Dimethyl-4''-[8'''-(2''',5'''-benzoquinonyl)-1'-naphthyl]-10,20-diphenylporphyrin (2b).** A dry CH<sub>2</sub>Cl<sub>2</sub> solution of **10b** (33 mg, 0.032 mmol) was cooled to -78 °C, following which 10 equivalents of BBr<sub>3</sub> (324 μL of a 1.0 M CH<sub>2</sub>Cl<sub>2</sub> solution, 0.32 mmol) were added dropwise. The reaction was stirred for 1 h at -78 °C and then slowly warmed to room temperature. After stirring for two additional h, a small quantity of methanol was added, and the reaction stirred for an additional 15 min. The reaction was partitioned between CH<sub>2</sub>Cl<sub>2</sub> and saturated Na<sub>2</sub>CO<sub>3</sub>. The organic layer was washed with saturated Na<sub>2</sub>CO<sub>3</sub> (3 × 20 mL) dried, and filtered; PbO<sub>2</sub> (100 mg) was added, and the heterogeneous CH<sub>2</sub>Cl<sub>2</sub> solution was stirred for 30 min. After filtering and removal of the volatiles, the red material was chromatographed on silica gel (CH<sub>2</sub>Cl<sub>2</sub>). After consolidation of the product fractions, **2b** was isolated as a glassy red solid; yield = 12 mg (40% based on 33 mg of compound **10b**). *anti:syn* 1.3:1 <sup>1</sup>H NMR (250 MHz, CDCl<sub>3</sub>, see Figure 2 for proton labeling schematic): δ 10.24 (s'', 1 H, H<sub>meso</sub>), 10.20 (s', 1 H, H<sub>meso</sub>), 9.41 (d', 1 H, *J* = 4.7 Hz, H<sub>β</sub>), 9.37 (d'', 1 H, *J* = 5.0 Hz, H<sub>β</sub>), 9.33 (d'', 1 H, *J* = 4.9 Hz, H<sub>β</sub>), 9.25 (d', 1 H, *J* = 4.5 Hz, H<sub>β</sub>), 9.04 (d', 1 H, *J* = 4.7 Hz, H<sub>β</sub>), 8.98 (d'', 1 H, *J* = 4.2 Hz, H<sub>β</sub>), 8.90 (d'', 1 H, *J* = 4.4 Hz, H<sub>β</sub>), 8.85 (d', 1 H, *J* = 5.5 Hz, H<sub>β</sub>), 8.77 (d'', 1 H, *J* = 4.0 Hz, H<sub>β</sub>), 8.75 (d', 1 H, *J* = 4.0 Hz, H<sub>β</sub>), 8.66 (d', 2 H, *J* = 4.7 Hz, H<sub>β</sub>), 8.61 (d'', 1 H, *J* = 4.9 Hz, H<sub>β</sub>), 8.54 (d'', 1 H, *J* = 4.7 Hz, H<sub>β</sub>), 8.49 (d'', 1 H, *J* = 4.8 Hz, H<sub>β</sub>), 8.38 (d, 1 H, *J* = 7.8 Hz, H<sub>11</sub>), 8.33 (d', 1 H, *J* = 5.0 Hz, H<sub>β</sub>), 8.27–8.06 (m, 4 H), 7.99–7.90 (m, 2 H), 7.84–7.63 (m, 8 H, H<sub>12</sub> + H<sub>meta/para</sub>, 10,20 phenyls + H<sub>15</sub>), 7.37 (d'', 1 H, *J* = 8.5 Hz, H<sub>8</sub>), 7.34 (d', 1 H, *J* = 8.4 Hz, H<sub>8</sub>), 7.02–6.79 (m, 3 H, H<sub>9</sub> + H<sub>7</sub> + H<sub>16</sub>), 6.54 (d'', 1 H, *J* = 7.0 Hz, H<sub>10</sub>), 6.51 (d', 1 H, *J* = 7.3 Hz, H<sub>10</sub>), 6.20 (dd', 1 H, *J* = 2.8 Hz, *J* = 10.0 Hz, H<sub>17</sub>-Quinone), 6.15 (dd'', 1 H, *J* = 2.7 Hz, *J* = 10.6 Hz, H<sub>17</sub>-Quinone), 5.98 (d', 1 H, *J* = 9.8 Hz, H<sub>18</sub>), 5.77 (d'', 1 H, *J* = 10.0 Hz, H<sub>18</sub>), 5.56 (d', 1 H, *J* = 2.7 Hz, H<sub>19</sub>), 5.53 (d'', 1 H, *J* = 2.9 Hz, H<sub>19</sub>), 5.42 (s'', 1 H, H<sub>6''-xylene</sub>), 5.19 (s', 1 H, H<sub>6''-xylene</sub>), 4.68 (t, 1 H, *J* = 7.6 Hz, H<sub>6</sub>), 4.32 (s'', 1 H, H<sub>3''-xylene</sub>), 4.30 (s', 1 H, H<sub>3''-xylene</sub>), 1.47 (s', 3 H, Me), 1.37 (s'', 3 H, Me), 0.53 (d'', 1 H, *J* = 7.6 Hz, H<sub>5</sub>), 0.51 (d', 1 H, *J* = 5.4 Hz, H<sub>5</sub>), -0.89 (s'', 3 H, Me), -1.25 (s', 3 H, Me), -1.98 (s (br), 1 H, N–H), -2.04 (s (br), 1 H, N–H). Vis (CH<sub>2</sub>Cl<sub>2</sub>): 422 (5.38), 516 (4.09), 552 (3.71), 591 (3.65), 646 (3.47). HRMS (ESI<sup>+</sup>) *m/z*: 925.3498 (calcd for C<sub>66</sub>H<sub>45</sub>N<sub>4</sub>O<sub>2</sub> (M + H) 925.3543).

**5-[8'-(2'',5''-Difluoro-4''-[8'''-(2''',5'''-benzoquinonyl)-1'-naphthyl]-10,20-diphenylporphyrin (2c).** A dry CH<sub>2</sub>Cl<sub>2</sub> (5 mL) solution of **10c** (11 mg, 0.011 mmol) was cooled to -78 °C, following which 10 equiv of BBr<sub>3</sub> (100 μL of a 1.0 M CH<sub>2</sub>Cl<sub>2</sub> solution, 0.1 mmol) were added dropwise. The reaction was stirred for 1 h at -78 °C, and then slowly warmed to room temperature. After stirring for an additional h, a small quantity of methanol was added, and the reaction stirred for an additional 15 min. The reaction was partitioned between CH<sub>2</sub>Cl<sub>2</sub> and saturated Na<sub>2</sub>CO<sub>3</sub>. The organic layer was washed with saturated Na<sub>2</sub>CO<sub>3</sub> (3 × 20 mL) dried, and filtered; PbO<sub>2</sub> (100 mg) was added, and the heterogeneous CH<sub>2</sub>Cl<sub>2</sub> solution was stirred for 30 min. After filtering and removal of the volatiles, the red material was chromatographed on silica gel (CH<sub>2</sub>Cl<sub>2</sub>). The product was collected as the first red band. After consolidation of the product fractions, **2c** was isolated as a glassy red solid; yield = 3.9 mg (39% based on 11 mg of compound **10c**). *anti:syn* 5.1:1 <sup>1</sup>H NMR (500 MHz, CDCl<sub>3</sub>, see Figure 2 for proton labeling schematic): δ 10.24 (s'', 1 H, H<sub>meso</sub>), 10.22 (s', 1 H, H<sub>meso</sub>), 9.40 (d', 1 H, *J* = 4.5 Hz, H<sub>β</sub>), 9.37 (d'', 1 H, *J* = 4.6 Hz, H<sub>β</sub>), 9.31 (d'', 1 H, *J* = 4.5 Hz, H<sub>β</sub>), 9.25 (d', 1 H, *J* = 4.7 Hz, H<sub>β</sub>), 9.04 (d', 1 H, *J* = 4.6 Hz, H<sub>β</sub>), 9.00 (d'', 1 H, *J* = 4.5 Hz, H<sub>β</sub>), 8.90 (m, 1 H, H<sub>β</sub>), 8.83 (d', 1 H, *J* = 4.5 Hz, H<sub>β</sub>), 8.80 (d', 1 H, *J* = 4.8 Hz, H<sub>β</sub>), 8.73 (d'', 1 H, *J* = 4.8 Hz, H<sub>β</sub>), 8.63 (d'', 1 H, *J* = 4.8 Hz, H<sub>β</sub>), 8.58 (d', 1 H, *J* = 4.6 Hz, H<sub>β</sub>), 8.51 (d'', 1 H, *J* = 4.8 Hz, H<sub>β</sub>), 8.39 (dd, 1 H, *J* = 1.2 Hz, *J* = 8.1 Hz, H<sub>11</sub>), 8.31 (dd, 1 H, *J* = 1.3 Hz, *J* = 8.4 Hz, H<sub>14</sub>), 8.28–8.26 (m, 1 H, H<sub>ortho</sub>, 10,20 phenyls), 8.21–8.20 (m, 2 H, H<sub>13</sub> + H<sub>β</sub>), 8.15 (d' (br), 2 H, H<sub>ortho</sub>, 10,20 phenyls), 8.08 (d'' (br), 2 H, H<sub>ortho</sub>, 10,20 phenyls), 7.91 (d'' (br), 1 H, H<sub>ortho</sub>, 10,20 phenyls), 7.88 (d' (br), 1 H, H<sub>ortho</sub>, 10,20 phenyls), 7.84 (t', 1 H, *J* = 7.5 Hz, H<sub>12</sub>), 7.83 (t'', 1 H, *J* = 7.5 Hz, H<sub>12</sub>), 7.78–7.60 (m, 7 H, H<sub>15</sub> + H<sub>meta/para</sub>, 10,20 phenyls), 7.32 (dd, 1 H, *J* = 1.1 Hz, *J* = 8.2 Hz, H<sub>8</sub>), 6.98 (t, 1 H, *J* = 8.2 Hz, H<sub>9</sub>), 6.95 (dd'',

1 H,  $J = 1.1$  Hz,  $J = 6.9$  Hz,  $H_{16/7}$ , 6.93 (dd', 1 H,  $J = 1.1$  Hz,  $J = 6.9$  Hz,  $H_{16/7}$ ), 6.89 (dd'', 1 H,  $J = 1.1$  Hz,  $J = 8.6$  Hz,  $H_{16/7}$ ), 6.85 (dd', 1 H,  $J = 1.1$  Hz,  $J = 7.2$  Hz,  $H_{16/7}$ ), 6.60 (d'', 1 H,  $J = 1.1$  Hz,  $J = 6.9$  Hz,  $H_{10}$ ), 6.57 (dd', 1 H,  $J = 1.1$  Hz,  $J = 6.8$  Hz,  $H_{10}$ ), 6.25 (dd'', 1 H,  $J = 2.5$  Hz,  $J = 10.3$  Hz,  $H_{17}$ -Quinone), 6.24 (dd', 1 H,  $J = 2.5$  Hz,  $J = 10.0$  Hz,  $H_{17}$ -Quinone), 6.00 (d'', 1 H,  $J = 10.0$  Hz,  $H_{18}$ -Quinone), 5.94 (d', 1 H,  $J = 10.0$  Hz,  $H_{18}$ -Quinone), 5.89–5.88 (m, 1 H,  $H_{19}$ -Quinone), 5.64 (d'', 1 H,  $J = 2.5$  Hz,  $H_{19}$ -Quinone), 5.53 (dd'', 1 H,  $J = 6.2$  Hz,  $J = 9.2$  Hz,  $H_{6''}$ -difluorophenyl), 5.43 (dd', 1 H,  $J = 6.0$  Hz,  $J = 9.2$  Hz,  $H_{6''}$ -difluorophenyl), 4.60 (t'', 1 H,  $J = 7.1$  Hz,  $H_6$ ), 4.50 (t', 1 H,  $J = 7.1$  Hz,  $H_6$ ), 3.95 (dd'', 1 H,  $J = 6.0$  Hz,  $J = 8.9$  Hz,  $H_{3''}$ -difluorophenyl), 3.85 (dd', 1 H,  $J = 6.0$  Hz,  $J = 8.8$  Hz,  $H_{3''}$ -difluorophenyl), 0.56 (d (br), 1 H,  $J = 6.8$  Hz,  $H_5$ ), 0.40 (dd', 1 H,  $J = 1.1$  Hz,  $J = 6.9$  Hz,  $H_5$ ), -3.19 (s (br), 2 H, N–H).  $^{19}\text{F}$  NMR (200 MHz,  $\text{CDCl}_3$ ):  $\delta$  -116.62 (d', 1 F,  $J = 13.8$  Hz), -117.90 (m'', 1 F), -121.77 (d', 1 F,  $J = 15.8$  Hz), -123.19 (d'', 1 F,  $J = 16.2$  Hz). Vis ( $\text{CH}_2\text{Cl}_2$ ): 420 (5.40), 515 (4.08), 548 (3.64), 589 (3.64), 645 (3.49). HRMS ( $\text{ESI}^+$ )  $m/z$ : 933.3070 (calcd for  $\text{C}_{64}\text{H}_{39}\text{F}_2\text{N}_4\text{O}_2$  (M + H) 933.3041).

## Results and Discussion

**Design.** Several criteria were considered in the design of these D–Sp–A systems. For example, to potentially assess how the nature of quadrupolar interactions and the magnitude of interplanar separations between stacked aromatic entities impact the magnitude of D–A electronic coupling in these  $\pi$ -cofacially aligned ET systems, a rigorously rigid D–Sp–A assembly is required. These D–Sp–A compounds stand in sharp contrast to previously synthesized porphyrin- and quinone-based ET systems in which flexible tethers hold porphyrin and quinonyl moieties at distances greater than or equal to the sum of their respective van der Waals radii.<sup>6,11,15,38–41</sup> Likewise, tethered P–Q assemblies that are structurally reminiscent of archetypal cyclophane compounds<sup>42–46</sup> do not preclude dynamical processes that modulate the magnitude of inter-ring separation or the extent of the lateral shift<sup>47</sup> between aromatic units on the photoinduced charge separation and thermal charge recombination time scales and hence complicate detailed analyses of ET rate data obtained in such systems.

The synthetic challenge of covalently linking multiple (>2) arene units in a closely held cofacial  $\pi$ -stacked arrangement is formidable; few molecular designs meet this requirement, which is underscored by the fact that traditional routes to cyclophane architectures make difficult the design and synthesis of such systems. Recent work by Wartini and Neugebauer exploited the [2.2] paracyclophane motif to investigate intramolecular charge delocalization between cofacial aromatic units using electrochemical and electron paramagnetic resonance methods.<sup>48–50</sup>

(37) Ishiyama, T.; Murata, M.; Miyaura, N. *J. Org. Chem.* **1995**, 60, 7508–7510.

(38) Ganesh, K. N.; Sanders, J. K. M. *J. Chem. Soc., Perkin Trans. 1* **1982**, 1611.

(39) Leighton, P.; Sanders, J. K. M. *J. Chem. Soc., Chem. Commun.* **1984**, 856.

(40) Abraham, R. J.; Leighton, P.; Sanders, J. K. M. *J. Am. Chem. Soc.* **1985**, 107, 3472.

(41) Sessler, J. L.; Johnson, M. R.; Creager, S. E.; Fetting, J. C.; Ibers, J. A. *J. Am. Chem. Soc.* **1990**, 112, 9310–9329.

(42) Weiser, J.; Staab, H. A. *Angew. Chem., Int. Ed. Engl.* **1984**, 23, 623.

(43) Weiser, J.; Staab, H. A. *Tetrahedron Lett.* **1985**, 26, 6059–6062.

(44) Staab, H. A.; Weikard, J.; Ruckemann, A.; Schwogler, A. *Eur. J. Org. Chem.* **1998**, 2703, 3–2712.

(45) Staab, H. A.; Kratzer, B.; Quazzotti, S. *Eur. J. Org. Chem.* **1998**, 2149–2160.

(46) Staab, H. A.; Hauck, R.; Popp, B. *Eur. J. Org. Chem.* **1998**, 631, 1–642.

(47) Scheidt, R. W.; Lee, Y. J. *Struct. Bonding* **1987**, 64, 1–70.

(48) Wartini, A. R.; Staab, H. A.; Neugebauer, F. A. *Eur. J. Org. Chem.* **1998**, 1161–1170.

(49) Wartini, A. R.; Valenzuela, J.; Staab, H. A.; Neugebauer, F. A. *Eur. J. Org. Chem.* **1998**, 221, 1–227.

In these assemblies, the arene-based electrophores are held at an interplanar separation of 3.1 Å, 0.3 Å below the van der Waals contact distance<sup>51</sup> for two cofacial aromatics. While these systems do in fact enforce a sub-van der Waals interplanar separation between juxtaposed arenes, systematic modulation of the electronic structure of the components of these assemblies, as well as the expansion of this motif to multiple levels of  $\pi$ -stacking interactions, clearly define arduous synthetic tasks. Due to the modular nature of the route exploited in the fabrication of  $\pi$ -stacked compounds **1** and **2a–c**, (Schemes 1–3) structure–function relationships that determine the magnitude of D–A electronic coupling can be more readily probed.

Compounds **1** and **2a–c** highlight the utility of the simple and versatile 1,8-diarylnaphthalene molecular scaffold in the fabrication of D–Sp–A systems designed to interrogate how electronic interactions that derive from  $\pi$ -stacking effects impact D–A electronic coupling. Seminal work by House<sup>36</sup> and Roberts<sup>52–54</sup> detailed the molecular structure of 1,8-diphenylnaphthalene; X-ray crystallographic studies show that these compounds typically manifest a structure in which the two aryl rings are held in a cofacial arrangement with a torsional angle of approximately 70° with respect to the naphthalene plane. Because these compact structures manifest considerable electrostatic repulsion between the compressed  $\pi$ -aromatic systems, the two aryl units splay outward, resulting in an enlargement of the naphthalene C(1)–C(9)–C(8) angle by approximately 5°. The effect of this splaying of the aryl moieties is also apparent in the differing distances that separate the C(1) and C(8) carbon atoms of the naphthalene ring (2.563 Å), and the C(1') aryl carbon atoms of the 1,8-diphenyl substituents (2.993 Å). Congruently, the naphthalene carbon framework exhibits distorted bond lengths and angles, the most notable of which are the displacements of the C(1) (–0.012 Å) and C(8) (+0.017 Å) atoms from the naphthalene least-squares plane. Despite these sterically driven deformations of the naphthalene bridge, it is noteworthy that the inter-planar separation between the C(1') atoms of the cofacial 1,8-aryl substituents is ~0.4 Å less than the arene–arene van der Waals contact distance.

The substantial geometric constraints imposed by the 1,8-naphthalene skeleton make this unit an ideal scaffold upon which to elaborate an extensive series of model compounds to probe the nature of electronic interactions in  $\pi$ -stacked arene systems. As a case in point, Cozzi and Siegel have carried out detailed nuclear magnetic resonance studies that correlate the magnitude of arene ring rotational barriers with phenyl-ring-substituent Hammett parameters; this work evinced the dominance of polar- $\pi$  effects over charge-transfer (CT) interactions in determining the extent of  $\pi$ - $\pi$  delocalization in 1,8-diarylnaphthalene systems,<sup>55–58</sup> and highlighted the degree to which nuclear dynamics can be attenuated in a  $\pi$ -stacked D–A system that takes advantage of a 1,8-naphthyl pillaring motif. Given the

(50) Wartini, A. R.; Valenzuela, J.; Staab, H. A.; Neugebauer, F. A. *Eur. J. Org. Chem.* **1998**, 139, 9–148.

(51) Pauling, L. *The Nature of the Chemical Bond*, 3rd ed.; Cornell University Press: Ithaca, NY, 1960.

(52) Clough, R. L.; Kung, W. J.; Marsh, R. E.; Roberts, J. D. *J. Org. Chem.* **1976**, 41, 3603–3609.

(53) Clough, R. L.; Roberts, J. D. *J. Am. Chem. Soc.* **1976**, 98, 1018–1020.

(54) Clough, R. L.; Roberts, J. D. *J. Org. Chem.* **1978**, 43, 1328–1331.

(55) Cozzi, F.; Cinquini, M.; Annunziata, R.; Dwyer, T.; Siegel, J. S. *J. Am. Chem. Soc.* **1992**, 114, 5729–5733.

(56) Cozzi, F.; Cinquini, M.; Annunziata, R.; Siegel, J. S. *J. Am. Chem. Soc.* **1993**, 115, 5330–5331.

(57) Cozzi, F.; Ponzini, F.; Annunziata, R.; Cinquini, M.; Siegel, J. S. *Angew. Chem., Int. Ed. Engl.* **1995**, 34, 1019–1020.

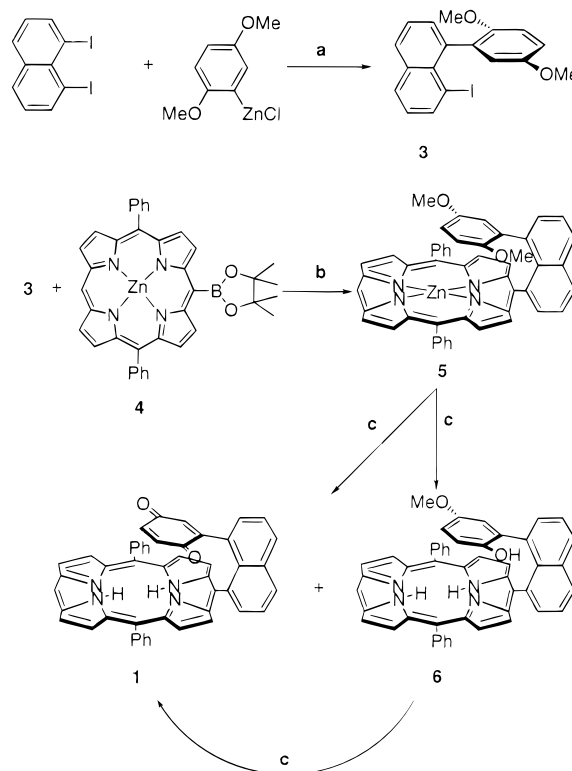
(58) Cozzi, F.; Siegel, J. S. *Pure Appl. Chem.* **1995**, 67, 683–689.

size of the porphyrin macrocycle and the fact that multiple, substantial dynamical restraints are enforced by a 1,8-diarylnaphthyl backbone, it is expected that combination of a porphyrin basal unit with 1,8-naphthyl linkers should give rise to D–Sp–A systems (**1**, **2a–c**) featuring structural rigidity that exceeds that evinced in analogous 1,8-naphthyl-linked phenylenes for identical levels of  $\pi$  stacking.

From a synthetic perspective, the availability of 1,8-dihalonaphthalenes<sup>36,59–62</sup> allows exploitation of metal-catalyzed cross-coupling strategies in the fabrication  $\pi$ -stacked D–Sp–A systems that feature naphthyl scaffolds linking successive aromatic moieties; notably in this regard, 1,8-diarylnaphthalene syntheses have been accomplished previously via Ni(II)-catalyzed coupling reactions utilizing Grignard reagents,<sup>52,53,59,63</sup> as well as by Ullmann coupling.<sup>36,55,56</sup> Corresponding Suzuki-type synthetic routes to such compounds have also appeared in the literature,<sup>64–66</sup> given both the versatility and facile reaction conditions of the Suzuki reaction we chose to build structures **1** and **2a–c** using a modular synthetic approach based on a family of aryl halide, porphyrinyl bromide,<sup>34,35</sup> arylboronate,<sup>37,67,68</sup> and porphyrinyl boronic acid ester reagents.<sup>14</sup>

**Synthesis.** Schemes 1–3 highlight the reagents, coupling protocols, and reaction conditions that were employed in the syntheses of compounds **1** and **2a–c**. Modified Suzuki conditions,<sup>28,29,69,70</sup> developed for systems in which hydrolytic deboronation is a significant side reaction, were required for many of the coupling reactions outlined herein. This cross-coupling protocol is carried out under anhydrous conditions, employing a dry polar solvent (DMF) and weakly soluble base ( $K_3PO_4$ ); all carbon–carbon bond-forming reactions involving the 1-iodo-8-arylnaphthalenic substrate were carried out under these conditions, which effectively suppressed deleterious dehalogenation and deboronation processes.

Interestingly, the modified Suzuki conditions described above were not effective in coupling reactions involving [5-(4',4',5',5'-tetramethyl[1',3',2']dioxaborolan-2'-yl)-10,20-diphenylporphyrinato]zinc(II) **4** and dimethoxy-protected naphthyl halide substrates such as **3** (Scheme 1) or **9a–c** (Scheme 2). If, however, conventional Suzuki conditions that utilize strongly basic conditions (aqueous  $Ba(OH)_2$ ) are employed, coupling proceeds in good yield. The presence of hydroxide ions, however, does result in observable deboronation of the porphyrinic transmetalating reagent in this sterically encumbered cross-coupling reaction.<sup>68,69</sup> In a typical experiment, it was found that an excess of porphyrinyl boronic ester **4** (1.5–2.0 equiv) was sufficient to compensate for any loss of this reagent due to hydrolytic deboronation over the time scale of the metal-catalyzed cross-coupling reaction.

**Scheme 1<sup>a</sup>**

<sup>a</sup> Key: (a)  $Pd(Ph_3)_4$ , THF, rt (61%); (b)  $Ba(OH)_2 \cdot 8H_2O$ ,  $Pd(Ph_3)_4$ , DME/ $H_2O$ , 80 °C (92%); (c) (i)  $BBr_3$ ,  $C_6H_6$ , rt; (ii)  $Na_2CO_3$  (aq).

Aryl diboronic esters **7a–c** proved to be key building blocks in the fabrication of compounds **2a–c**. Such diboronic acids and their respective ester derivatives have been exploited in the synthesis of terphenyl compounds, fused polycyclic aromatic compounds,<sup>71</sup> and sugar conjugates,<sup>68</sup> and have typically been prepared by transmetalation of a halogenated aromatic starting material and subsequent reaction with trialkoxyboron reagents;<sup>72–75</sup> after hydrolysis, the conversion of the resulting diboronic acid derivative to the corresponding diboronic ester is accomplished via simple esterification.<sup>76</sup>

Recently, Miyaura and Masuda have reported alternative routes to synthesize arene diboronic ester compounds,<sup>37,67</sup> which exploit Pd-catalyzed coupling reaction of bis(pinacolato)-diboron<sup>37</sup> or dialkoxyhydroborane<sup>67</sup> species with halogenated aromatics. This methodology not only provides a direct, one-step conversion of dihaloaryl compounds to their corresponding diboronic ester derivatives; it enables the high yield preparation of arylboronates in the presence of functional groups sensitive to strong base, and circumvents the need to isolate and characterize the corresponding diboronic acid derivatives.<sup>68</sup> The wide range of commercially available 1,4-dihalogenated arene precursors coupled with Miyaura and Masuda methodology allows for the facile introduction of a variety of intervening aromatic moieties that differ in their respective electronic and

(59) Kuroda, M.; Nakayama, J.; Hoshino, M.; Furusho, N.; Kawata, T.; Ohba, S. *Tetrahedron* **1993**, 49, 3735–3748.

(60) Letsinger, R. L.; Gilpin, J. A.; Vullo, W. J. *J. Org. Chem.* **1962**, 27, 672–674.

(61) Kiely, J. S.; Nelson, L.; Boudjouk, P. J. *J. Org. Chem.* **1977**, 42, 1480.

(62) Fieser, L. F.; Seligman, M. J. *Am. Chem. Soc.* **1939**, 61, 136–142.

(63) Cosmo, R.; Sternhell, S. *Aust. J. Chem.* **1987**, 40, 1107–1126.

(64) Bahl, A.; Grahn, W.; Stadler, S.; Feiner, F.; Bourhill, G.; Brauchle, C.; Reisner, A.; Jones, P. G. *Angew. Chem., Int. Ed. Engl.* **1995**, 34, 1485–1488.

(65) Zoltewicz, J. A.; Maier, N. M.; Fabian, W. M. F. *J. Org. Chem.* **1997**, 62, 3215.

(66) Zoltewicz, J. A.; Maier, N. M.; Fabian, W. M. F. *Tetrahedron* **1996**, 52, 8703–8706.

(67) Murata, M.; Watanabe, S.; Masuda, Y. *J. Org. Chem.* **1997**, 62, 6458–6459.

(68) Todd, M. H.; Balasubramanian, S.; Abell, C. *Tetrahedron Lett.* **1997**, 38, 6781–6784.

(69) Suzuki, A. *Pure Appl. Chem.* **1994**, 66, 213–222.

(70) Watanabe, T.; Miyaura, N.; Suzuki, A. *Synlett* **1992**, 207–210.

(71) Goldfinger, M. B.; Crawford, K. B.; Swager, T. M. *J. Am. Chem. Soc.* **1997**, 119, 4578–4593.

(72) Clement, R.; Champetier, G. *C. R. Acad. Sci. Paris (C)* **1966**, 1398–1400.

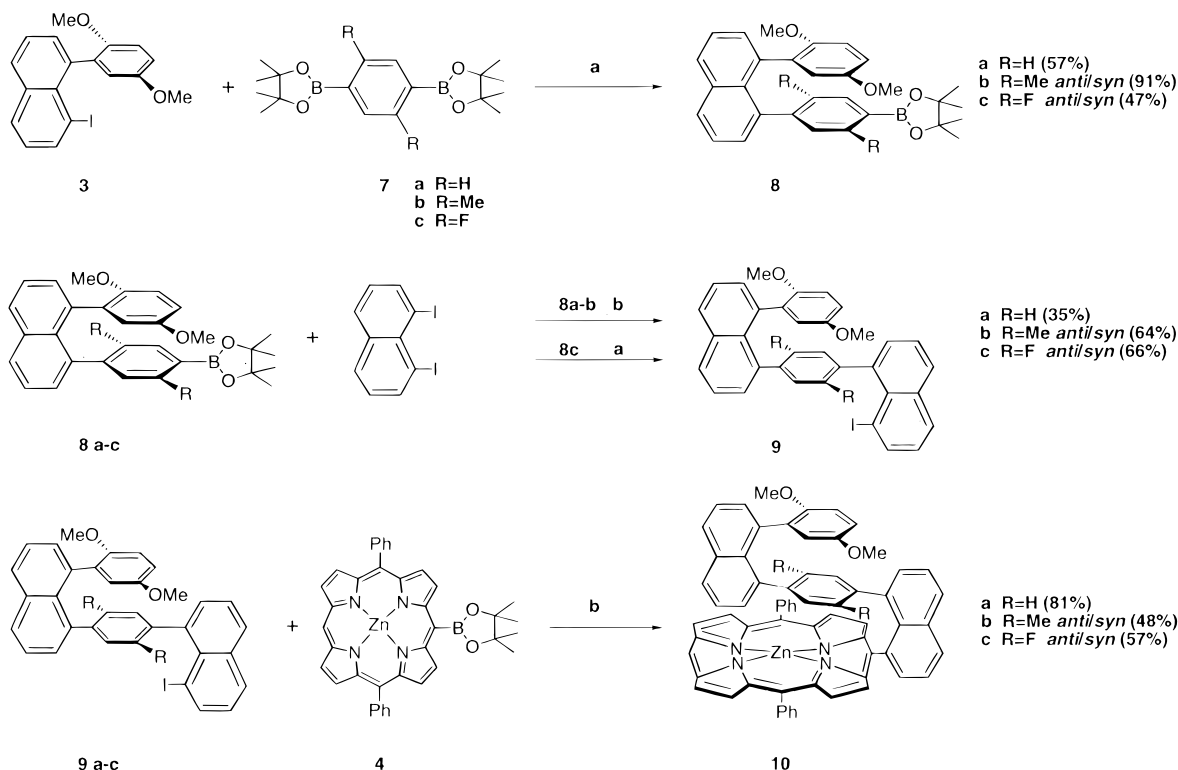
(73) Musgrave, O. C. *Chem. Ind.* **1957**, 1152.

(74) Nielsen, D. R.; McEwan, W. E. *J. Am. Chem. Soc.* **1957**, 79, 3081–3084.

(75) Coutts, I. G. C.; Goldschmid, H. R.; Musgrave, O. C. *J. Chem. Soc., C* **1970**, 488–493.

(76) Waas, J. R.; Sidduri, A. R.; Knochel, P. *Tetrahedron Lett.* **1992**, 33, 3717–3720.



Scheme 2<sup>a</sup>

<sup>a</sup> Key: (a)  $K_3PO_4$ ,  $Pd(Ph_3)_4$ , DMF, 100 °C; (b)  $Ba(OH)_2 \cdot 8H_2O$ ,  $Pd(Ph_3)_4$ , DME/ $H_2O$ , 80 °C.

steric properties between porphyrin and quinone in compound 2-type structures. The one-to-one coupling of 1,4-diboronate ester derivatives 7a–c (Scheme 2) with 1-iodo-8-(2,5-dimethoxyphenyl)naphthalene 3 gives compounds 8a–c, which notably retain boronic acid ester functionality at the 4' position of the naphthalene-1-aryl substituent, enabling further elaboration of these building blocks to give compounds 9a–c.

The synthesis of the 1-iodo-8-(2,5-dimethoxyphenyl)naphthalene (3, Scheme 1) relies on the stoichiometric reaction of 1,8-diiodonaphthalene with 2,5-dimethoxyphenylzinc chloride, employing standard Negishi cross-coupling protocols.<sup>31</sup> The reaction proceeds smoothly at ambient temperature and yields mono-aryl-substituted 3 in 57% yield. Under these reaction conditions, significant dehalogenation of the starting material does not occur, enabling any unreacted 1,8-diiodonaphthalene to be recovered. After successful monoarylation of the naphthyl *peri* position, the iodide remaining at the 1 position becomes extremely labile, due likely to the substantial steric crowding enforced by the naphthyl 8-dimethoxyphenyl substituent. Successful Suzuki coupling of 1,4-diboronate esters 7a–c at this sensitive position was only realized when the reaction was carried out in anhydrous DMF in the presence of phosphate base.<sup>29,69,70</sup> Other coupling protocols<sup>29,77</sup> developed for arylboronic acid and arylboronate transmetalating reagents gave dehalogenated 1-(2,5-dimethoxyphenyl)naphthalene as the sole product for reactions involving 3 and 7a–c.

As shown in Scheme 2, the coupling of substrate 3 with 1,4-diboronate esters 7a–c under weakly basic conditions generates  $\pi$ -stacked 1-(4-[4',4',5',5'-tetramethyl[1',3',2']dioxaborolan-2'-yl]aryl)-8-(2,5-dimethoxyphenyl)naphthalene structures 8a–c. As expected, the isolated 8b and 8c products exist as a mixture of *syn* and *anti* isomers. The *syn* isomer (Figure 1a) is characterized by an eclipsed orientation of the methoxy sub-

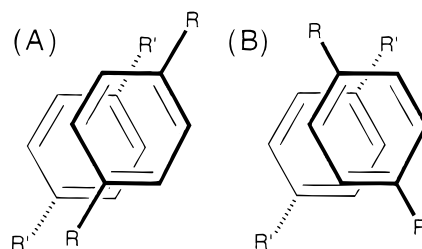


**Figure 1.** Top-down representations of the *syn* (A) and *anti* (B) diastereomers of 1,8-di[(2,5-disubstituted)aryl]naphthalenes.

stituents on the 8-aryl ring with the methyl (8b) or fluoro substituents (8c) of the phenyl ring attached to the naphthyl 1-position. Congruent with earlier reports that detail the syntheses of 1,8-diarylnaphthalenes featuring 2',5'-substituted phenyl groups,<sup>53,55</sup> the *anti* isomer (Figure 1b) is the major component of the diastereomeric mixture due to the reduced steric repulsions associated with a staggered orientation of the naphthyl 1- and 8-aryl substituents.

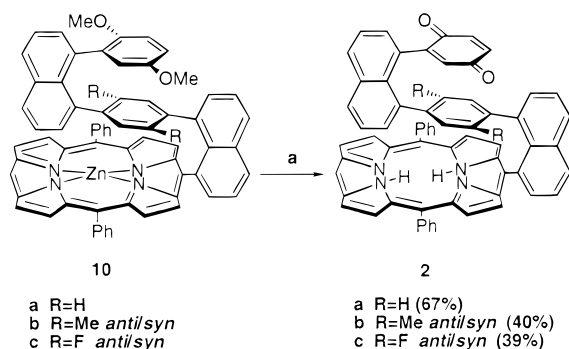
Similar to that observed for 8b–c, compounds 10b–c, and quinone products 2b–c are isolated as a mixture of *syn* and *anti* diastereomers. The observed *anti:syn* diastereomeric ratios for xylyl-spacer containing compounds 10b and 2b are similar (1.8:1 and 1.3:1, respectively). The corresponding *anti:syn* diastereomeric ratios for the analogous difluorophenyl-bridged species 10c and 2c are 3.3:1 and 5.1:1, respectively.<sup>78</sup>

The conversion of compounds 10a–c (Scheme 3) to their corresponding quinoidal derivatives was accomplished using the standard deprotection–oxidation protocol.<sup>79–83</sup> Treatment of

(78) The degree to which *syn/anti* diastereomerism affects conformational dynamics as well as donor–acceptor electronic coupling will be discussed elsewhere.

(79) Vickery, E. H.; Pahler, L. F.; Eisenbraun, E. J. *J. Org. Chem.* **1979**, *44*, 4444–4446.

(77) Kowitz, C.; Wegner, G. *Tetrahedron* **1997**, *53*, 15553–15574.

Scheme 3<sup>a</sup>

<sup>a</sup> Key: (a) (i) BBr<sub>3</sub>, CH<sub>2</sub>Cl<sub>2</sub>, rt; (ii) Na<sub>2</sub>CO<sub>3</sub> (aq); (iii) PbO<sub>2</sub>, CH<sub>2</sub>Cl<sub>2</sub>, rt.

porphyrin–spacer–dimethoxybenzene species **10a–c** with the demethylating agent BBr<sub>3</sub> followed by subsequent aqueous work up affords the intermediate hydroquinone derivatives, which can then be isolated and oxidized with PbO<sub>2</sub>. In contrast, this simple deprotection–oxidation sequence proved ineffective for compound **5** (Scheme 1), possibly due to a combination of factors that include: (i) the limited allowed dynamical motions of the two stacked aromatic moieties relative to each other that derives from the sub van der Waals interplanar separation between the 2,5-dimethoxyphenyl group and the larger porphyrin ring system, and (ii) the cavity like structure created by the three flanking porphyrin *meso* substituents (2 phenyl rings and 1 naphthyl unit), which limits access to the methoxy group oxygens by the demethylating reagent. Congruent with this latter point, (Figure 3), <sup>1</sup>H NMR chemical shift data (vide infra) for the three highly shielded dimethoxyphenyl protons ( $\delta$  = 4.88, 3.13, 2.42 ppm) and the two methoxy groups ( $\delta$  = 2.20, 1.26 ppm) indicate a time-averaged structure in which the dimethoxyphenyl ring is canted toward the porphyrin core, thereby orienting one of the methoxy substituents in the porphyrin cavity and causing the other such group to be more heavily solvated.

As shown in Scheme 1, treatment of **5** with excess BBr<sub>3</sub> generates monodemethylated compound **6** and a trace amount of quinone **1**. Resubjecting the monomethoxy species **6** to the BBr<sub>3</sub> deprotection (Scheme 1), enables small amounts of the benzoquinonyl derivative (**1**) of compound **5** to be generated (7%). The hydroquinone intermediate air oxidizes to the product porphyrin–quinone complex **1** as it is formed; no attempt was made to elucidate reaction conditions that would enable the isolation of 5-[8'-(2'',5''- dihydroxyphenyl)-1'-naphthyl]-10,20-diphenylporphyrin.

**Structural Comparisons with 1,8-Diarylnaphthalene Benchmarks.** Dynamical studies that probe the extent to which rotation is hindered in 1,8-diarylnaphthalenes<sup>36,63</sup> and analogous asymmetrically substituted species<sup>59,65,66,84</sup> have been used as a tool to probe the factors important in determining the strength of  $\pi$ – $\pi$  interactions.<sup>55–58</sup> The interconversion of *anti* and *syn* isomers requires a 180° rotation by one of the aryl ring substituents; the transition state for this process is generally assumed to feature one phenyl substituent in the naphthalene

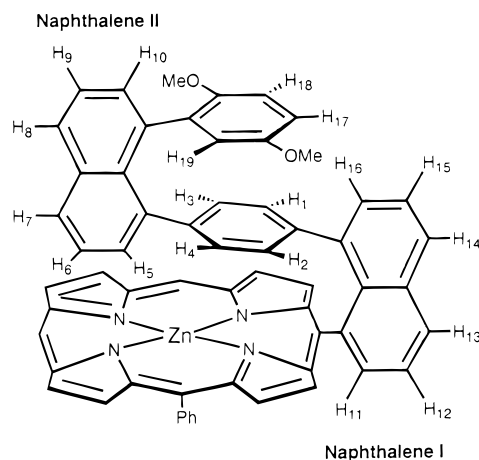


Figure 2. Proton labeling schematic for compound **10a**.

plane with the other aryl ring fixed orthogonal to it.<sup>63</sup> In this model, the outward splaying of the 1,8-diaryl groups serves to reduce the steric interactions between *meta* substituents of the juxtaposed phenyl groups, while unavoidable, severe steric clashes occur if *ortho* substituents are present on these rings. Both calculated and experimentally derived rotational barriers<sup>53–56</sup> demonstrate that the magnitude of  $\Delta G^\ddagger$  for such a rotation in a 1,8-diarylnaphthalene structure is considerably higher when the phenyl-ring substituents occupy *ortho* positions.

Because such rotational barriers are increased substantially in simple *ortho*-substituted 1,8-diarylnaphthalenes (e.g.,  $\Delta G^\ddagger$  (1,8-di-*o*-tolyl)naphthalene) = 24.1 kcal/mol<sup>53,55</sup> relative to that determined for 1,8-diphenyl naphthalene and *meta*-substituted 1,8-diarylnaphthalenes (e.g.,  $\Delta G^\ddagger$  (1-(3'-isopropylphenyl)-8-phenylnaphthalene) = 16.4 kcal/mol),<sup>54,63</sup> steric arguments dictate that compounds **5** and **10a–c** should possess considerably augmented barriers to aryl ring rotation relative to that elucidated for 1,8-diphenyl naphthalenes, due to the presence of a basal porphyrin unit in these  $\pi$ -stacked ET systems. Factors responsible for the rigidifying effect that the porphyrin unit has in these systems can be seen in the atom-labeled **10a** structure shown in Figure 2. The positioning and relative orientation of naphthalenes I and II (Figure 2) function synergistically to augment rotational barriers of their respective aryl and porphyrin substituents. For example, from the perspective of the (porphyrinato)zinc(II) moiety, the C <sub>$\beta$</sub>  carbon atoms that flank the porphyrin *meso* carbon fused to naphthalene I's 1-position constitute effective *ortho* substituents; porphyrin ring rotations are thus coupled to steric clashes involving the corresponding porphyrin C <sub>$\beta$</sub>  protons with the H<sub>11</sub> atom of naphthalene I. While such interactions would be expected to enforce rotational barriers similar to that observed for *ortho*-substituted 1,8-diarylnaphthalenes, it is crucial to note that naphthalene II also serves to restrict rotation of the (porphyrinato)zinc(II) unit about the C<sub>*meso*</sub>-to-C<sub>1-Naphthyl</sub> bond; any porphyrin ring librating motion causes enhanced steric clashes with naphthalene II's H<sub>6</sub> and H<sub>5</sub> atoms with the macrocycle plane; consistent with such a conformational restraint playing a key role in restricting nuclear dynamics, it is worth emphasizing at this point that the time-averaged positions of H<sub>5</sub> and H<sub>6</sub> account for two of the most dramatic <sup>1</sup>H NMR signatures observed for compounds **2a–c** (vide infra).

**NMR Spectroscopy.** The 1-D <sup>1</sup>H NMR spectral data obtained for the porphyrin–(protected quinone) complexes (**5** and **10a–c**) as well as the porphyrin–quinone charge-transfer systems (**1** and **2a–c**) are noteworthy (Figures 3 and 4). The rigid geometry coupled with the sub-van der Waals interplanar separations manifest in these porphyrin-based D–Sp–A systems

(80) Chan, A. C.; Dalton, J.; Milgrom, L. R. *J. Chem. Soc., Perkin Trans. 2* **1982**, 2.

(81) McIntosh, A. R.; Siemiarz, A.; Bolton, J. R.; Stillman, M. J.; Ho, T. F.; Weedon, A. C. *J. Am. Chem. Soc.* **1983**, *105*, 7215–7223.

(82) Schmidt, J. A.; Siemiarz, A.; Weedon, A. C.; Bolton, J. R. *J. Am. Chem. Soc.* **1985**, *107*, 6112–6114.

(83) Zhang, Y.; Hoernfeldt, A.-B.; Gronowitz, S. *J. Heterocycl. Chem.* **1995**, *32*, 435–444.

(84) Zoltewicz, J. A.; Maier, N. M.; Fabian, W. M. F. *J. Org. Chem.* **1996**, *61*, 7018–7021.



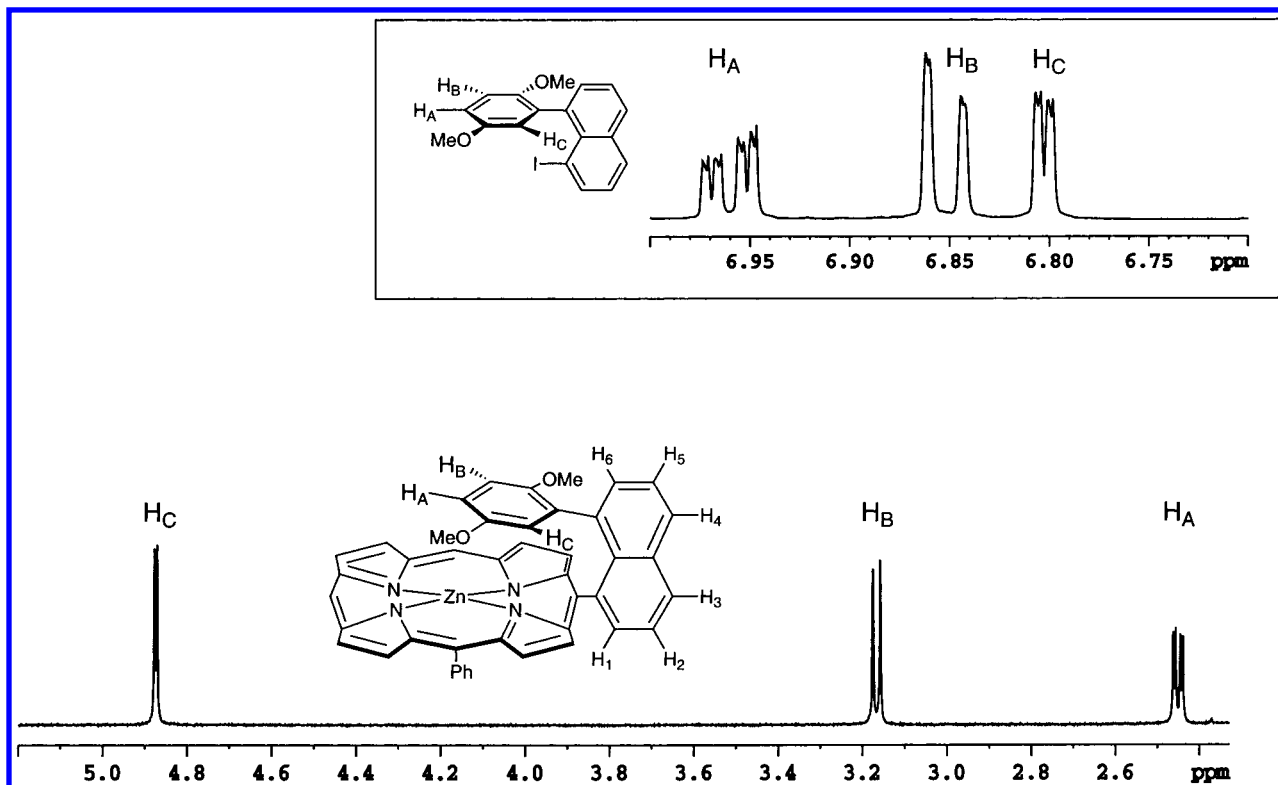


**Figure 3.** Upfield region of the 500 MHz  $^1\text{H}$  NMR spectrum of [5-(8'-(2'',5''-dimethoxyphenyl)-1'-naphthyl)-10,20-diphenylporphinato]zinc(II) **5** in  $\text{CDCl}_3$  at room temperature. The inset shows the  $^1\text{H}$  NMR spectrum of the dimethoxyphenyl region of precursor molecule **3**. The 20-phenyl substituent on the porphyrin ring has been omitted for clarity.

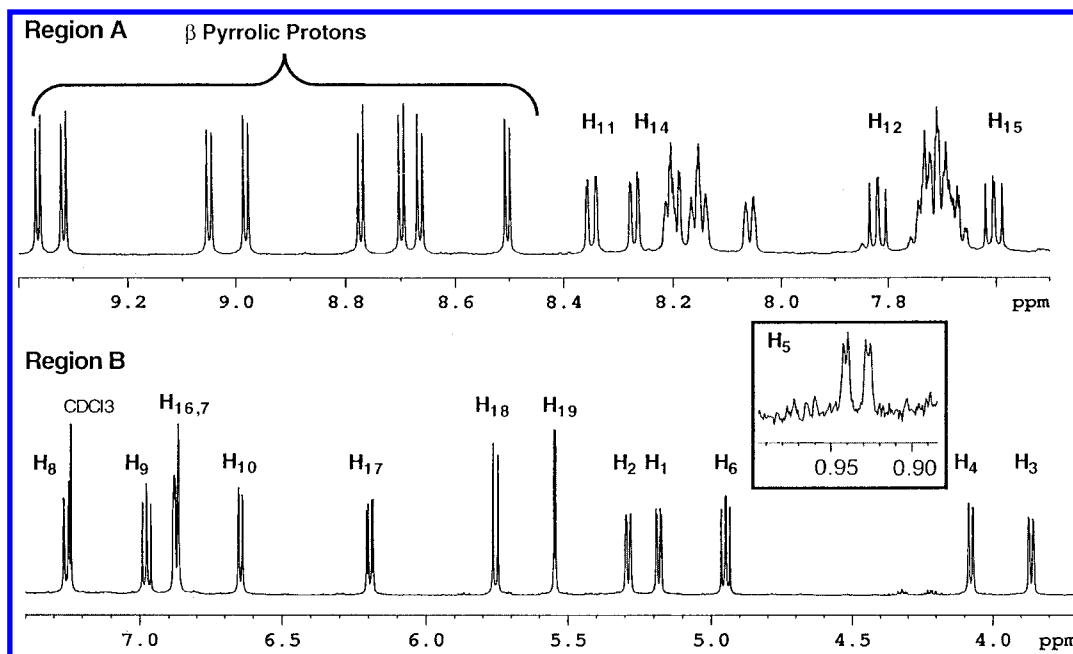


**Figure 4.** 500 MHz  $^1\text{H}$  NMR spectrum of [5-(8'-[4''-(8'''-[2''', 5'''-dimethoxyphenyl]-1')-1''-phenyl]-1'-naphthyl)-10,20-diphenylporphinato]zinc(II) (**10a**) in  $\text{CDCl}_3$ . The proton labeling scheme is described in Figure 2.

gives rise to disparate shielding effects which distribute the aromatic  $^1\text{H}$  resonances for these species over wide spectral windows.

Such unusually large shielding effects are apparent in compound **5**'s  $^1\text{H}$  NMR spectrum, the upfield region of which is shown in Figure 3. This spectrum shows a number of signatures that differ from the analogous  $^1\text{H}$  NMR spectra of compounds **8a–c** and related 1,8-diarylnaphthalenes. Most striking is the large upfield shift observed for the three

dimethoxyphenyl ring protons of **5** relative to the  $\text{H}_\text{A}$ ,  $\text{H}_\text{B}$ , and  $\text{H}_\text{C}$  proton resonances of 1-iodo-8-(2,5-dimethoxyphenyl)naphthalene (**3**) which exhibit chemical shift values of 6.96, 6.85, and 6.80 ppm respectively (Figure 3, inset). After cross-coupling compound **3** with the porphyrin boronate complex **4**, the  $\text{H}_\text{A}$ ,  $\text{H}_\text{B}$ , and  $\text{H}_\text{C}$  dimethoxy aryl proton signals of **5** shift upfield to 2.43, 3.13, and 4.88 ppm respectively; note that the shielding effect experienced by  $\text{H}_\text{A}$  in **5** is particularly pronounced ( $\Delta\delta = 4.53$  ppm with respect to the analogous resonance of **3**). Note

also that the methoxy protons are shielded by the porphyrin aromatic  $\pi$  system; in the precursor molecule **3**, the methoxy resonances are located at  $\delta = 3.79$  and 3.65 ppm, while in porphyrin compound **5** they are observed to resonate at  $\delta = 2.20$  and 1.26 ppm. Congruently, the  $^1\text{H}$  NMR spectrum of the cofacial porphyrin–quinone complex **1** shows that the three quinonoid protons resonate at chemical shifts of  $\delta = 1.65$ , 2.02, and 4.97 ppm, while the benchmark  $^1\text{H}$  chemical shift value for 1,4-benzoquinone lies substantially downfield at  $\delta = 6.83$  ppm.

Given the relative structural simplicity of **5** in this series of porphyrin-based stacked aromatic structures, variable temperature  $^1\text{H}$  NMR spectroscopic studies (data not shown) were performed in order to estimate the minimum barrier height for rotation of the 1,8-naphthyl moiety's porphyrin and 2,5-dimethoxyphenyl substituents. Compound **5** has eight assignable  $\beta$ -proton resonances (Experimental Section). Free rotation of the porphyrin and aryl naphthalene substituents on the NMR time scale would result in the coalescence of symmetry related pairs of these  $\beta$ -proton signals to give four resonances. Interestingly, the  $^1\text{H}$  NMR spectrum of **5** recorded at 120 °C is virtually identical to the ambient temperature spectrum; the only NMR time scale dynamics evident correlate with librations and rotations of the porphyrin 10- and 20-phenyl substituents.<sup>85–87</sup> All of the  $\beta$ -proton resonances remain sharp, with their chemical shift values unperturbed relative to the spectrum recorded at 30 °C. Selecting a pair of well-resolved  $\beta$  proton resonances that would be chemically equivalent in the advent of free rotation of the 2,5-dimethoxyphenyl moiety that exhibited the smallest chemical shift difference at 30 °C provides an estimate for the activation barrier for rotation of at least 22 kcal/mol<sup>88</sup> in these porphyrin-based  $\pi$ -stacked systems. Three conclusions can be drawn from this analysis: (i) the barrier to rotation in **5** is at a minimum comparable to that elucidated by Clough and Roberts<sup>53</sup> as well as Siegel and Cozzi<sup>55</sup> for 1,8-di-(*o*-tolyl)-naphthalene derivatives; (ii) replacing a simple phenyl ring with a porphyrin group in 1,8-diarylnaphthalene systems augments the rotational barrier height by at least 6 kcal/mol; and (iii) use of NMR techniques (such as 2-D EXSY<sup>89</sup>) will likely not be useful probes of rotational barriers in compounds related structurally to **5**.

More dramatic shielding effects are manifest in the spectra observed for tri-level  $\pi$ -stacked structures **10a–c** and **2a–c**. As a case in point, note that compound **10a** possesses a total of 44 protons, of which 38 are aromatic; remarkably, 38 of the 44 proton resonances are directly assignable in the 1-D spectrum. Note that only the signals for *meta* and *para* protons of the porphyrin 10- and 20-phenyl groups overlap (Figure 4). The aromatic resonances for **10a** have chemical shift values that range from 0.93 ppm ( $\text{H}_5$  in Figure 4) to 10.15 ppm (the porphyrin *meso* proton). Note the extraordinary spectral resolution evident in Figure 4, and the fact that analogous spectroscopic features are manifest in the 1-D  $^1\text{H}$  NMR spectra of the related **10b–c** and **2a–c** structures as well (Experimental Section; Supplementary Material).

Figure 4 divides the  $^1\text{H}$  NMR spectrum of compound **10a** into two regions labeled A and B; resonance assignments are denoted using the labeling scheme of Figure 2. Region A of the spectrum highlights primarily the porphyrinic resonances,

and include the signals corresponding to the *ortho* and *meta*, *para* protons of the porphyrin *meso*-phenyl substituents, as well as the resonances assigned to the naphthalene I pillar (Figure 2). Note that each of the porphyrin  $\beta$ -proton resonances exhibits a unique chemical shift, and appears as a well-resolved doublet within the 9.36–8.50 ppm spectral domain. The naphthalenic signals displayed in region A of Figure 4 ( $\text{H}_{11}$ – $\text{H}_{16}$ , Figure 2) resonate at chemical shift values close to that observed for simple 1,8-disubstituted naphthalenes, as expected, given that the protons on naphthalene I reside outside the porphyrin-shielding region.

In contrast, the naphthalenic resonances highlighted in region B (naphthalene II, Figure 2) of compound **10a**'s  $^1\text{H}$  NMR spectrum lie substantially upfield from the naphthalene I protons and are observed over a large spectral window (7.25–0.93 ppm). The signal corresponding to proton  $\text{H}_5$  (Figure 4) at 0.93 ppm is shifted upfield by approximately 6.5 ppm from the analogous resonance of compound **9a** and approximately 6.4 ppm from the corresponding resonance of compound **8a**; few, if any, diamagnetic aromatic compounds manifest shielding effects of this magnitude. The assignment of the 0.93 ppm doublet to the  $\text{H}_5$  nucleus was verified by a 500 MHz homonuclear COSY experiment;<sup>88</sup> this resonance displays a clear cross-peak to the triplet centered at 4.95 ppm ( $\text{H}_6$ ). The unusually large upfield shift experienced by  $\text{H}_5$  (and the corresponding resonances for compounds **10b–c** and **2a–c**) highlight the impact that the close, sub van der Waals separation between the porphyrin and the edge of the upright naphthalene II pillar has upon the local magnetic environment sampled by these nuclei (Figure 4); importantly, the assignment of the 0.93 ppm doublet to  $\text{H}_5$  coupled with the clear trend with respect to the degree of shielding experienced by the naphthalene II protons ( $\text{H}_5 \gg \text{H}_6 \gg \text{H}_7 > \text{H}_8, \text{H}_9, \text{H}_{10}$ ) provide important structural information regarding the orientation of naphthalene II relative to the porphyrin plane.

Compounds **10a–c** (**2a–c**) were engineered to provide a cofacial arrangement of porphyrin, spacer, and dimethoxy arene (quinone) at sub van der Waals interplanar separations while maintaining an approximately orthogonal arrangement of the planes of naphthalene pillars with respect to the porphyrin macrocycle. In such a structure, electronic interactions between the porphyrin, spacer, and dimethoxyarene (quinone) ring systems are presumably extensive, while electronic coupling between the naphthalene pillars and the cofacial aromatic moieties is minimized due to unfavorable  $\pi$  overlap. The 1-D  $^1\text{H}$  NMR spectroscopic data obtained for compounds **10a–c** and **2a–c** is consistent with expectations based on molecular modeling that naphthalene II will be forced to adopt an upright orientation. The  $^1\text{H}$  NMR data for these species manifest a distribution of resonances over a wide spectral window that derives from radically different magnetic environments sampled by their respective aromatic protons. Certainly, if the structure probed on the NMR time scale for molecules **2a–c** and **10a–c** were consistent with a relatively small dihedral angle between the porphyrin and naphthalene II least squares planes, one would expect to see a more clustered pattern of chemical shifts due to similar shielding effects experienced by the  $\text{H}_5$ – $\text{H}_{10}$  nuclei; this is inconsistent with the data presented in Figure 4 (compound **10a**) and analogous tabulated spectroscopic data presented in the Experimental Section and Supplementary Material for compounds **2a–c** and **10b–c**. Because both naphthalene pillars manifest an essentially perpendicular orientation with respect to the porphyrin least-squares plane, highly anisotropic shielding environments for these ring systems are assured, thereby

(85) Eaton, S. S.; Eaton, G. R. *J. Am. Chem. Soc.* **1975**, *97*, 3660–3666.

(86) Eaton, S. S.; Eaton, G. R. *J. Am. Chem. Soc.* **1977**, *99*, 6594–6599.

(87) Noss, L.; Lidell, P. A.; Moore, A. L.; Moore, T. A.; Gust, D. J. *Phys. Chem. B* **1997**, *101*, 458–465.

(88) Iovine, P. M.; Veglia, G.; Furst, G. T.; Therien, M. J. Manuscript in preparation.

(89) Perrin, C. L.; Dwyer, T. J. *Chem. Rev.* **1990**, *90*, 935–967.

enabling facile and unambiguous assignment of the  $^1\text{H}$  NMR spectra of compounds **2a–c** and **10a–c**.

Additional aspects of the 1-D  $^1\text{H}$  NMR spectrum of Figure 4 deserve further comment; note that the region B NMR signals feature resonances that are ascribed to the spacer moiety ( $\text{H}_1$ – $\text{H}_4$ ) and the dimethoxyphenyl ring ( $\text{H}_{17}$ – $\text{H}_{19}$ ) protons. The  $\text{H}_1$ ,  $\text{H}_2$ ,  $\text{H}_3$ , and  $\text{H}_4$  phenyl protons are shifted significantly upfield by 2.09, 1.98, 3.41, and 3.19 ppm with respect to the proton resonance frequency of benzene (7.27 ppm). Importantly, resonances  $\text{H}_1$ – $\text{H}_4$  are extraordinarily sharp, indicating that the central  $\pi$ -stacked phenyl ring of compound **10a** remains static on the NMR time scale. The dimethoxyphenyl ring ( $\text{H}_{17}$ – $\text{H}_{19}$ ) protons, likewise, by virtue of the sub van der Waals, cofacial arrangement of the phenyl and dimethoxyaryl ring systems, are shielded relative to analogous aromatic resonances of compound **3** by 0.76, 1.10, and 1.25 ppm, respectively. These shielding effects derive from the respective magnetic contributions of the neighboring cofacial phenyl spacer and the aromatic porphyrin moiety, as well as conformational constraints that limit nuclear dynamics of the 2,5-dimethoxyphenyl moiety in **10a** relative to simple 1,8-aryl-substituted naphthyl derivatives. Comparison of the relative resonance frequencies for the dimethoxyphenyl arene protons of compounds **8a**, **3**, and **10a** demonstrates that the approximate shielding contribution from the phenyl moiety only accounts for 0.58, 0.67, and 0.25 ppm of the upfield shifts manifest by **10a**'s respective  $\text{H}_{17}$ ,  $\text{H}_{18}$ , and  $\text{H}_{19}$  hydrogen atoms. Perturbations to the local magnetic environment that emanate from the porphyrin ring current and a more rigid structure account for the additional respective 0.18, 0.43, and 1.0 ppm shielding experienced by  $\text{H}_{17}$ – $\text{H}_{19}$  nuclei of **10a** relative to that manifest by the analogous nuclei in compound **8a**.

### Summary and Conclusions

A prototype series of rigid  $\pi$ -stacked porphyrin–spacer–quinone (P–Sp–Q) systems have been synthesized; these systems differ in key respects from assemblies designed previously to probe the extent of electronic coupling afford by cofacial alignment of aromatic donor, bridge, and acceptor moieties. The 1,8-diarylnaphthalene pillaring motif, coupled with the presence of a basal porphyrin moiety, ensures significant molecular rigidity in these D–Sp–A systems and limits conformational heterogeneity in solution. These constructions fix sub van der Waals separations between juxtaposed donor, spacer, and acceptor units; as such, these systems will likely manifest increased  $\pi$  orbital electronic mixing between the

D–Sp–A system components in photoinduced electron transfer and thermal charge recombination reactions.

The 1-D  $^1\text{H}$  NMR experiments described herein evince that the 1,8-naphthyl moieties cofacially align aromatic D, Sp, A units and constrain the nuclei to reside in unusual and diverse local magnetic environments. The quality of the NMR data obtained for these assemblies of stacked aromatic residues is unusually high, due in part to the fact that diamagnetic aromatic proton NMR signals are spread over spectral windows that exceed 9.0 ppm; these exceptional  $^1\text{H}$  NMR spectra enable straightforward assignment of a high percentage of the aromatic resonances in these D–Sp–A assemblies.<sup>90</sup>

The modular synthetic approach outlined herein, that exploits metal-catalyzed cross-coupling methodologies<sup>29–35</sup> and the porphyrin boronate synthon<sup>14</sup> is well suited for systematic modification of electronic and steric properties of the donor, bridge, and acceptor components of these cofacial ET assemblies. Of equal importance, this synthetic strategy allows for control over the absolute energetics of the spacer bonding and antibonding states, as well as the nature of the quadrupolar interactions that exist between adjacent aromatic entities in these  $\pi$ -stacked assemblies; this flexibility to engineer a wide range of electronic factors in these systems while simultaneously enforcing sub van der Waals contacts and eliminating lateral shift between juxtaposed, cofacial aromatic moieties, distinguishes these D–Sp–A compounds from other classes of  $\pi$ -stacked structures synthesized and probed to date.

**Acknowledgment.** M.J.T. is indebted to the United States Department of Energy (DE-FG02-94ER14494) for their generous financial support of this work, and thanks the Alfred P. Sloan and Camille and Henry Dreyfus Foundations for research fellowships.

**Supporting Information Available:** Syntheses and characterization data for compounds **8b–c**, **9b–c**, and **10b–c**, as well as  $^1\text{H}$  NMR spectra for compounds **1**, **2a–c**, **5**, and **10a–c** are available (PDF). This material can be obtained free of charge via the Internet at <http://pubs.acs.org>.

JA000759A

(90) These facts, coupled with the observed sharp  $^1\text{H}$  resonances and the plethora of short through space proton–proton distances manifest in these structures, allow rigorous solution-phase structural determinations for these species as a function of temperature via modern NMR methods. See ref 88.